Zoological Journal of the Linnean Society, 2024, **202**, zlae106
https://doi.org/10.1093/zoolinnean/zlae106
Advance access publication 5 October 2024
Original Article

OXFORD

Original Article

Validity of *Myobradypterygius hauthali* von Huene, 1927 (Ichthyosauria: Ophthalmosauria) from the Early Cretaceous of Chile and Argentina

Judith Pardo-Pérez[1,2,*], Patricio Zambrano[3], Matthew Malkowski[4], Dean Lomax[5,6], Rodrigo Villa-Martínez[1,2], Wolfgang Stinnesbeck[7], Eberhard Frey[8], Francisca Scapini[1,2], Cristina Gascó[9] and Erin E. Maxwell[9]

[1]Centro de Investigación GAIA-Antártica, Universidad de Magallanes, Avenida Bulnes 01855, Punta Arenas, 6200000, Chile
[2]Cape Horn International Center (CHIC), Teniente Muñoz 166, Puerto Williams, Chile
[3]Septos Asesorías Geológicas, Avenida Costanera 7488, San Pedro de la Paz, Concepción, 4130000, Chile
[4]Department of Earth and Planetary Sciences, Jackson School of Geosciences, University of Texas at Austin, 2275 Speedway Stop C9000, Austin, TX 78712-1722, USA
[5]Palaeobiology Research Group, School of Earth Sciences, University of Bristol, Life Sciences Building, Tyndall Avenue, Bristol BS8 1TQ, UK
[6]Department of Earth & Environmental Sciences, University of Manchester, Oxford Road, Manchester M13 9PL, UK
[7]Instutut für Geowissenschaften, Universität Heidelberg, Im Neuenheimer Feld 234-236 69120, Heidelberg, Germany
[8]Sonnenbergstrasse 27, 75189 Pforheim, Germany
[9]State Museum of Natural History, Rosenstein 1, 70191 Stuttgart, Germany

[*]Corresponding author. Centro de Investigación GAIA-Antártica, Universidad de Magallanes, Avenida Bulnes 01855, Punta Arenas, 6200000, Chile; Cape Horn International Center (CHIC), Teniente Muñoz 166, Puerto Williams, Chile. E-mail: judith.pardo@umag.cl

ABSTRACT

Early Cretaceous ichthyosaurs were globally distributed pelagic marine reptiles, but many remains are fragmentary, creating a Northern Hemisphere diversity bias. A rich Hauterivian locality near the Tyndall Glacier inside Torres del Paine National Park in southern Chile yields important new data regarding ichthyosaurian diversity along the Pacific margin of Gondwana. These new data will contribute to clarifying questions regarding ichthyosaur taxonomy and the palaeobiogeographical relationships between the southern Gondwanan and Northern Hemisphere ichthyosaur groups during the Early Cretaceous. Here, we describe three new ichthyosaur specimens from this locality. Two of them are referred to *Myobradypterygius hauthali*, expanding the distribution of this species from the Barremian of Argentina to the Hauterivian of the Chilean Patagonia. This material shows that *M. hauthali* differs from *Platypterygius platydactylus* in forefin construction and scapular morphology, supporting its classification as a separate genus within Platypterygiinae. The third specimen is a large-bodied indeterminate ophthalmosaurine ichthyosaur. This record represents the southernmost record of Ophthalmosaurinae and the first occurrence of this group from the Cretaceous of the Southern Hemisphere. These discoveries show that ophthalmosaurines and platypterygiines continued to occur sympatrically in southernmost Gondwana during the Early Cretaceous, expanding the pattern documented in Europe to the Pacific region.

Keywords: Ichthyosauria; Early Cretaceous; Gondwana; Patagonia

INTRODUCTION

Our understanding of the fossil record of pelagic tetrapods, including ichthyosaurs, is heavily influenced by the taphonomy, preservation, and excavation and by the accessibility of deep-water fossil lagerstätten (Benson and Butler 2011). In South America, this bias creates large gaps in the fossil record, with a few faunal assemblages adding significantly to our understanding of the diversity and evolution of Ichthyosauria in the Eastern Pacific and Proto-Caribbean regions.

In South America, ichthyosaurs are best documented from three key fossil lagerstätten spanning the Middle Jurassic–Early Cretaceous time period. In the Proto-Caribbean, the exceptional Barremian–Aptian assemblage from the Paja Formation has yielded two ichthyosaur genera to date, namely

Received 12 December 2023; revised 5 April 2024; accepted 14 August 2024
© The Author(s) 2024. Published by Oxford University Press on behalf of The Linnean Society of London. All rights reserved. For commercial re-use, please contact reprints@oup.com for reprints and translation rights for reprints. All other permissions can be obtained through our RightsLink service via the Permissions link on the article page on our site—for further information please contact journals.permissions@oup.com.

Muiscasaurus Maxwell *et al.* (2016) and *Kyhytysuka* Cortés *et al.* (2021), but at least four taxa were present (Cortés *et al.* 2023). More significantly, from the Eastern Pacific region, the slightly older and much better-studied Tithonian–Berriasian Vaca Muerta Formation from Argentina has yielded abundant ichthyosaurian material, which currently comprises five named genera [*Catutosaurus* Fernández *et al.* (2021), *Caypullisaurus* Fernández (1997), *Sumpalla* Campos *et al.* (2021), *Arthropterygius* Maxwell (2010), and *Ancanamunia* (Rusconi, 1940) (potential junior synonym of *Ophthalmosaurus*): Fernández 2007, Campos *et al.* 2020]. Lastly, the Los Molles Formation, also from the Eastern Pacific region of Argentina, has yielded rare but highly significant ichthyosaur remains of Middle Jurassic (Bajocian) age, including at least three taxa: *Chacaicosaurus*, *Mollesaurus*, and an unnamed genus (reviewed by Fernández and Talevi 2014).

A fourth unusual South American ichthyosaur-bearing fossil lagerstätte of Early Cretaceous age from the Zapata Formation, southern Chile has been reported in the literature (Pardo-Pérez *et al.* 2012, Stinnesbeck *et al.* 2014). Four taxa have been noted, referred to *Platypterygius hauthali* (von Huene, 1927), *Platypterygius* cf. *hauthali*, *Platypterygius* sp. 3, and Ophthalmosauridae indet. 1 (Stinnesbeck *et al.* 2014). However, the material has not been described adequately, and the taxonomic composition of the fauna is in need of careful evaluation. Here, we initiate this analysis for two of these taxa, '*Platypterygius*' *hauthali* and 'Ophthalmosauridae' indet. 1.

We provide a detailed description of this new material and a critical review of forefin anatomy of '*P.*' *hauthali* based on more complete remains. Additionally, we re-evaluate the specimen referred to Ophthalmosauridae indet. 1 by Stinnesbeck *et al.* (2014) and reassign it to Ophthalmosaurinae indet. Although we describe the specimen, the material is insufficiently exposed for taxonomic assignation to genus. We demonstrate conclusively that at least two generically distinct ichthyosaurs were present at the locality. These findings not only will provide crucial information for understanding latitudinal diversity gradients in ichthyosaurs in the Southern Hemisphere but also further illustrate the global significance of the Tyndall site.

Geological context

The Tyndall fossil locality, next to the Tyndall Glacier inside Torres del Paine National Park in the Magallanes region in southernmost Chile, has preserved nearly 100 ichthyosaur skeletons, most of them complete and articulated (Fig. 1).

Fossils are preserved within the Upper Jurassic to Early Cretaceous Zapata Formation, which is well exposed near the terminus of the Tyndall Glacier. The fossils have been revealed

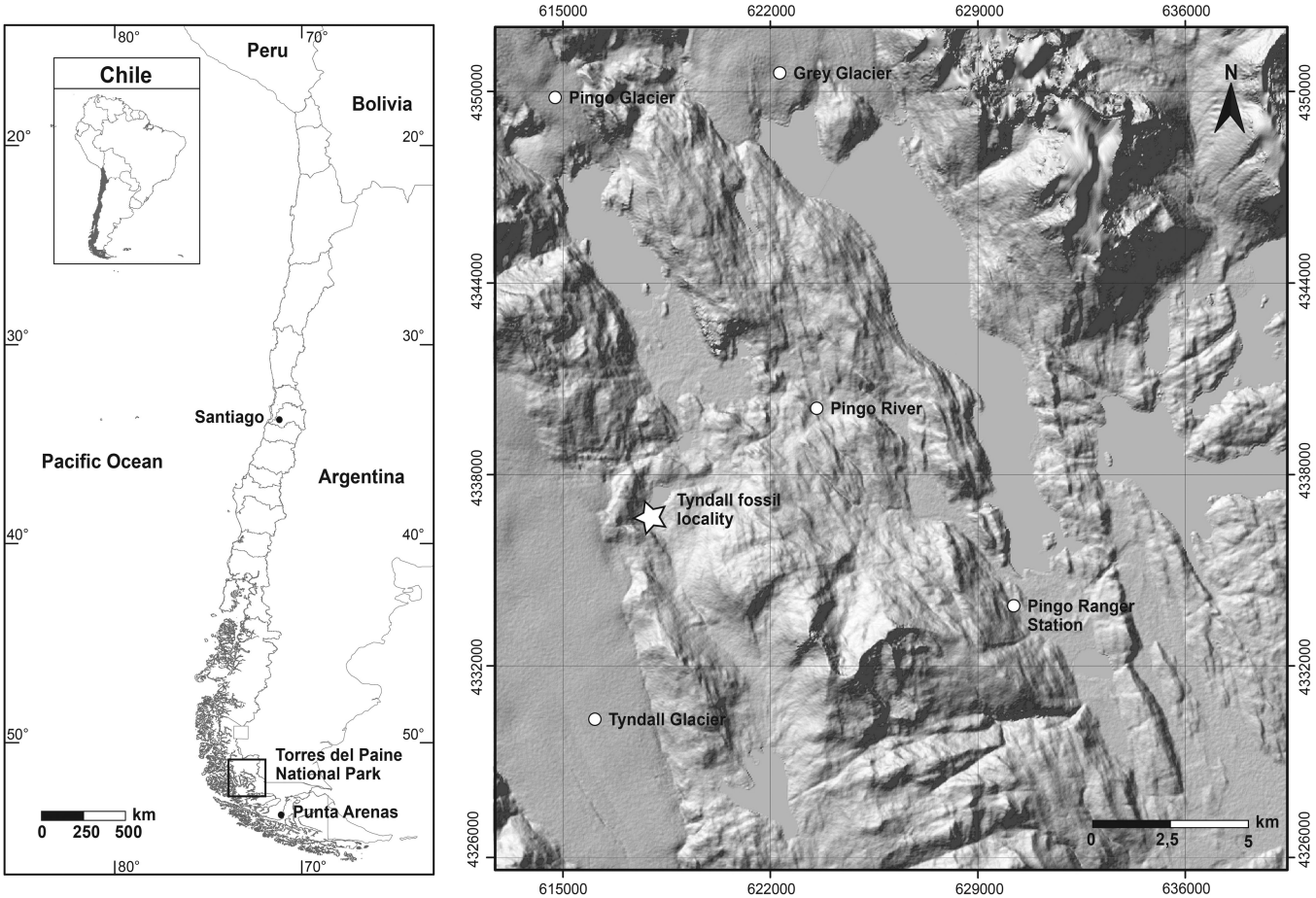

Figure 1. Geographical location of the fossil locality in the Torres del Paine National Park, southernmost Chile, Magallanes region. The digital elevation model (DEM) was downloaded from the free platform of Alaska Satellite Facility (ASF) Data Search from the University of Alaska System (https://search.asf.alaska.edu/). The downloaded images were processed using ArcGIS Desktop 10.5 and Illustrator (version 2022).

by the ongoing melt-off of the glacier in the past two decades, now exposing an area of ~15 km^2.

The Zapata Formation represents the predominantly fine-grained fill of the Rocas Verdes ocean basin, which opened diachronously, from south to north, in a back-arc extensional setting associated with the early break-up of Gondwana (Dalziel *et al.* 1974, Stern and de Wit 2003, Malkowski *et al.* 2016). At the study location, the Zapata Formation consists of a heterolithic assemblage of carbonaceous, calcareous, and siliceous mudstone interbedded with siltstone and very fine-grained sandstone units. Wilson (1991) subdivided these packages into five informal members (A–E). Most of the ichthyosaur skeletons and invertebrate-related fauna have been found within the 'D member' of the Zapata Formation, which consists of ~100 m of siliciclastic turbidites and alternating facies of (i) claystone and siltstone, (ii) sandstones, (iii) breccia, and (iv) injectites (Wilson 1991, Stinnesbeck *et al.* 2014). Ichthyosaur-bearing layers are commonly associated with tabular, thin- to medium-bedded (3–30 cm) sandstone facies reflecting submarine turbidity current deposits (Bouma 1962, Stinnesbeck *et al.* 2014). Compositionally, sandstone units are composed of feldspar, quartz, mica, minor mudstone rip-up clasts, and disseminated pyrite. Individual beds are normally grading from fine-grained sandstone to mudstone, containing planar laminations, ripples, and slumping levels. These facies are interpreted to represent internal divisions of turbidity current deposits (Bouma 1962). Bed scale slumping and soft sediment deformation are reflected in some intervals up to several metres thick, indicating a depositional setting with sufficient gradients to generate mass-transport deposits. From an architectural perspective, the alternation of these lithofacies with slump facies and mudstones might indicate either a position on the slope or a levee environment associated with submarine channels. However, the discontinuity of the outcrops, along with the mild deformation they exhibit, does not allow for a clear observation of the lateral relationships of these lithofacies.

To date, ichthyosaurs are the only marine reptiles discovered at Tyndall, but a diversity of ganoid and teleostean fishes was also present. The associated faunal assemblage composed of ammonites (*Favrella americana* Favre (1908), *Lissonia riveroi* (Lissón, 1907), and *Crioceratites diamantensis* Weaver (1931) *in* Gerth (1933), among others), inoceramid bivalves (*Neocomiceramus curacoensis* (Weaver, 1931), *Inoceramus*' sp. cf. *I. anomiaeformis* (Feruglio, 1936), and belemnites (*Belemenopsis* sp.) allows for an assignation of the ichthyosaur-bearing deposits to the Valanginian to Hauterivian age (139.8–125.77 Mya) (Stinnesbeck *et al.* 2014).

Recent U–Pb (Uranium-Lead) Chemical Abrasion through Termal ionization mass spectrometry (CA-TIMS) analyses of zircon from an ash bed near the base of the fossil-rich section indicate an age of 131.07 ± 0.07 Mya for the fossil-bearing deposits (M. Malkowski, pers. com., 2023). However, the geochronological analysis falls outside the scope of this article and will be addressed in a separate publication.

Institutional abbreviations

CPAP, Colecciones Paleontológicas de Antártica y Patagonia (Instituto Antártico Chileno, Punta Arenas, Chile) [Palaeontological Collection of Antarctic and Patagonia (Chilean Antarctic Institute, Punta Arenas, Chile)]; MHNRS, Museo de Historia Natural Río Seco, Punta Arenas, Chile [Natural History Museum Río Seco, Punta Arenas, Chile]; MLP, Museo de Ciencias Naturales de La Plata, Argentina [Museum of Natural Sciences from La Plata, Argentina]; SMNS, Staatliches Museum für Naturkunde Stuttgart, Stuttgart, Germany; TY, acronym for 'Tyndall', which is used to label non-excavated ichthyosaurs from the Tyndall fossil locality; UW, University of Wyoming, Laramie, WY, USA.

MATERIALS AND METHODS

Material

Three specimens from the Tyndall glacier fossil locality were used for this description (TY61, CPAP-2011-0019, and TY53). Given the previous referral to '*Platypterygius*' *hauthali* (hereafter referred to as *Myobradypterygius hauthali* von Huene, 1927), specimens were selected based on forefin preservation, which is diagnostic at the species level and allows detailed comparisons with the type material of this species. The third specimen, TY53, was selected owing to its unambiguous distinctiveness from the bulk of the previously determined material from the locality (*Myobradypterygius hauthali*, *Myobradypterygius* cf. *hauthali*, *Platypterygius* sp.; Pardo-Pérez *et al.* 2012, Stinnesbeck *et al.* 2014, Pardo-Pérez, 2015). Specimens are detailed as follows.

TY61: A complete and articulated skeleton preserving cranial and articulated postcranial material, partly exposed and >2.75 m long (total estimated length is 3 m). The skull is preserved in ventrolateral view and the postcranium in ventral view. The anterior rostrum is covered by sediment (Fig. 2). This specimen was discovered by Amaro Gómez-Pablos and Marcelo Arévalo in 2007 and remains *in situ*.

CPAP-2011-0019: An isolated and articulated forefin (Fig. 5D, E). This specimen was discovered by Patricio Zambrano in 2009. Currently, it is housed in the palaeontological collection of the Chilean Antarctic Institute in Punta Arenas, Chile.

TY53: A virtually complete, partly exposed specimen of ~5 m total estimated length. The exposed portion of the skeleton, from the skull to the end of the exposed caudal region, is 2.88 m long, preserving some cranial and postcranial elements. The specimen was discovered by Esteban Beltrán in 2009 and remains *in situ* (Fig. 6A, B).

Owing to the extremely hard matrix in which the Tyndall ichthyosaurs are enclosed, in addition to the remoteness of the locality, excavation is time consuming and logistically expensive. This has hampered the possibility of performing seasonal excavations in this area and limited the number of specimens collected. Specimen TY61 is scheduled as next to be excavated.

Methods

Specimens TY61 and TY53 were measured in the field using a measuring tape and callipers; detailed photographs were taken of each section. All specimens were drawn 1:1 on site with a water-permanent marker pen on a plastic acetate foil. For photogrammetry, we took a series of photographs from different angles, following the protocol outlined by Mallison and Wings (2014)

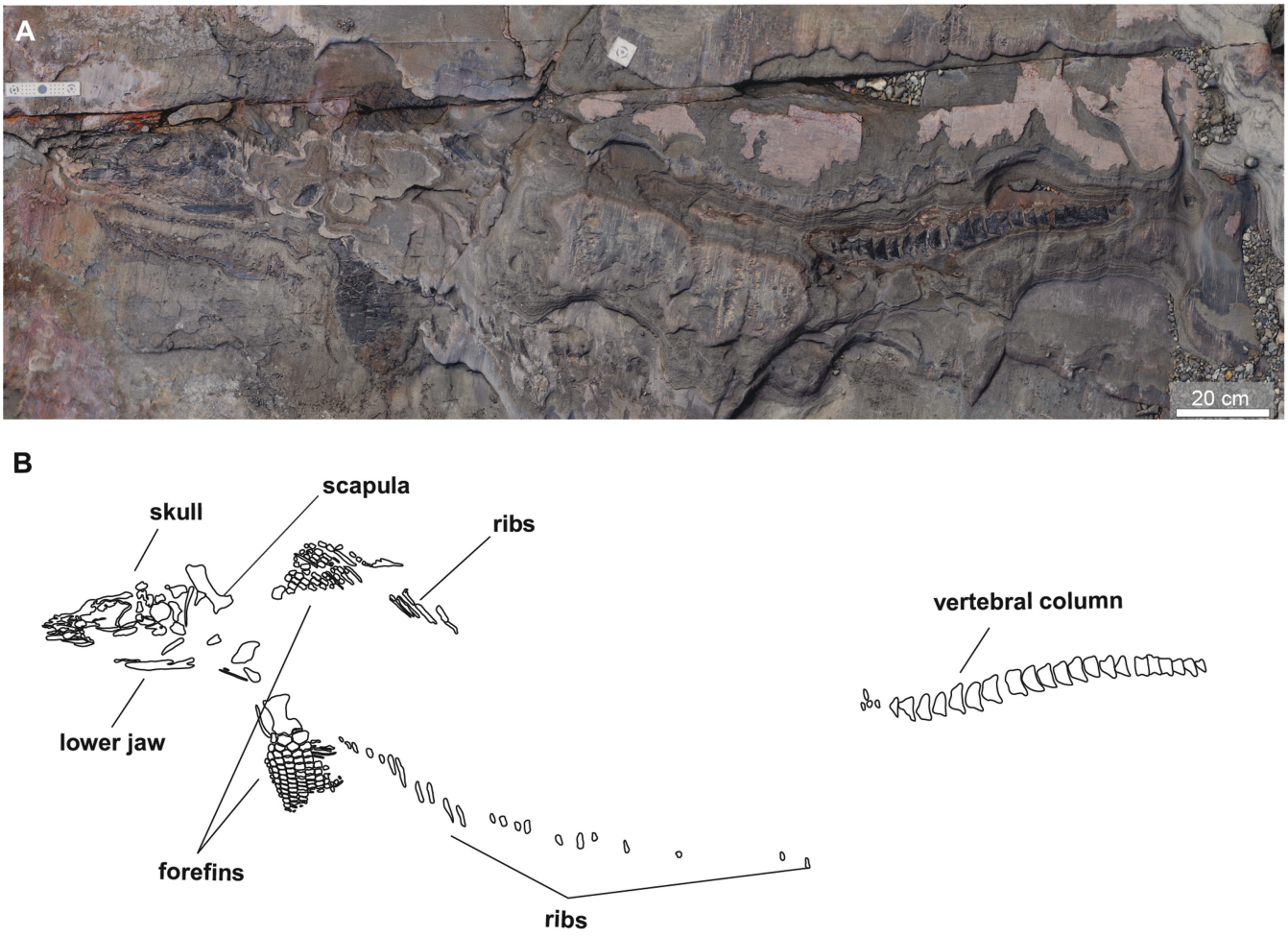

Figure 2. The complete skeleton of TY61. A, orthophotograph of the entire skeleton. B, interpretative drawing indicating the skeletal portions preserved and exposed.

and modified for field conditions following Mujal *et al.* (2020). The photogrammetric model was constructed using the software Meshroom (v.2021.1.0) (Griwodz *et al.* 2021), and refined in Meshlab v.2020.12 (Cignoni *et al.* 2008) (see Supporting Information, Supplementary files: 3D model S1 and S2).

For both *in situ* and excavated specimens, osteological details were assessed using a hand lens with ×10 magnification. Anatomical abbreviations were used following Moon and Kirton (2016).

Phylogenetic analysis

We scored *Myobradypterygius hauthali* in the character–taxon matrices of Campos *et al.* (2021) and Zverkov and Jacobs (2020), with *Thalassodraco* Jacobs and Martill (2020) added from Jacobs and Martill (2020), and Cortés *et al.* (2021), based solely on the Argentinean type material, TY61, and CPAP-2011-0019.

The resulting matrices were analysed using the software package TnT v.1.6 (Goloboff *et al.* 2023), based on an equal-weights maximum parsimony optimization criterion using a new technology search (ratchet = 50 iterations; find minimum tree 100 times). This was followed by a traditional search with trees from RAM. IterPCR (Pol and Escapa 2009) was used to prune unstable taxa from the resulting strict consensus tree; however, in general, this did not help to resolve the position of *Myobradypterygius hauthali* within Platypterygiinae further.

Implied weighting parsimony analysis has been found to outperform equal-weights parsimony for morphological datasets, providing a better-resolved topology (Goloboff *et al.* 2018). This better resolution comes at a cost, with a higher number of both correct and incorrect groupings; the desirability of the method hinges on the fact that more of the resolved groupings are correct than incorrect (Goloboff *et al.* 2018). In order to minimize the undesirable amplification of incorrect groupings relative to equal-weights parsimony, we used the extended implied weighting method, which counteracts the artificial upweighting of characters with a high proportion of missing data (Goloboff 2014). In addition, we collapsed nodes with an absolute score difference equivalent to one step in a character with homoplasy, as recommended by Goloboff *et al.* (2018); this value varies based on the selected *k*-value. This method also collapses some weakly supported correct nodes, but at a lower rate than incorrect nodes, and is therefore more conservative than the implementation practised by most authors (e.g. Laboury *et al.* 2022). In our opinion, minimization of incorrect nodes should be prioritized over topological resolution.

Selection of *k*-values remains one of the key difficulties of implied weighting parsimony, with the optimized topology varying considerably based on the concavity (*k*-value) selected. Goloboff *et al.* (2018) suggested that higher *k*-values ($k = 12$) performed better, 'especially with large datasets'. The correct *k*-value for a given dataset size remains undefined. The ophthalmosaurian dataset is very small, but given strong ecomorphological constraints on body plan in parvipelvian ichthyosaurs, the dataset has very high homoplasy, with clades defined by unique character combinations rather than unambiguous synapomorphies. For that reason, we selected a higher *k*-value ($k = 12$) than the size of the dataset alone might recommend, in order to avoid too severe downweighting of characters showing mild to moderate homoplasy. It should be noted that implied weighting can only optimize the best topology based on the data and remains affected by both quality of scoring and selection of operational taxonomic units (in terms of both taxa included and quality of the alpha taxonomy). IterPCR (Pol and Escapa 2009) was used to prune unstable taxa from the resulting strict consensus tree, when required. We applied extended implied weighting, as described above, to the three datasets analysed under equal weights; we also re-analysed the data of Campos *et al.* (2024) using extended implied weighting but without character re-scoring, in order to facilitate comparisons.

Higher-level clade names

Higher-level clade names are, at present, heavily debated for Late Jurassic and Cretaceous ichthyosaurs, with clade membership varying owing to both variable clade definitions and highly unstable phylogenetic results (e.g. Cortés *et al.* 2021, Zverkov 2022). Here, we use the following definitions:

Ophthalmosauria Motani, 1999 *sensu* Cortés *et al.* (2021): in this study, we include *Nannopterygius* and *Thalassodraco* in Ophthalmosauria; however some topologies recover these genera outside Ophthalmosauria (Cortés *et al.* 2021).

Ophthalmosaurinae *sensu* Fischer *et al.* (2012): Ophthalmosauridae, while having nomenclatural priority (Zverkov 2022), is well established in the literature as a synonym of Ophthalmosauria. Moreover, the clade as currently defined (*sensu* Cortés *et al.* 2021, Zverkov 2022) is highly unstable in phylogenetic analyses, with the result that the generic composition of the term varies enormously in the published literature. Given that it suits our purposes best with respect to the Tyndall material, we maintain Ophthalmosaurinae based on the diagnostic criteria advanced by Fischer *et al.* (2012), here understood as comprising a potentially non-monophyletic grouping of non-platypterygiine ophthalmosaurians including *Nannopterygius* and *Thalassodraco* in addition to the taxa comprising the core of this clade in the study by Fischer *et al.* (2012). As per the diagnosis of Fischer *et al.* (2012), *Arthropterygius* is excluded.

Platypterygiinae *sensu* Fischer *et al.* (2012): Bardet (1995) coined the name Platypterygiidae at the family level to comprise a clade including both *Nannopterygius* and *Grendelius* (=*Brachypterygius*). As such, Platypterygiidae should be considered a junior synonym of Ophthalmosauria, despite attempts to exclude *Nannopterygius* from the definition (Zverkov 2022). Arkhangelsky (1999) coined Platypterygiinae as a subfamily comprising all Cretaceous ichthyosaurs known at the time (*Platypterygius sensu* McGowan 1972); the subfamily was defined explicitly in 2001. In moving to a branch-based definition, Fischer *et al.* (2012) broadened the definition of the family substantially. Although this definition has been evaluated critically elsewhere (Cortés *et al.* 2021), it remains widely used and will be used here.

RESULTS

SYSTEMATIC PALAEONTOLOGY

Order Ichthyosauria de Blainville, 1835

Family Ophthalmosauria Montani, 1999

Subfamily Platypterygiinae Arkhangelsky, 2001

Genus *Myobradypterygius* von Huene, 1927 (Nace, 1939)

***Myobradypterygius hauthali* von Huene, 1927**

Diagnosis: (Expanded from that of Fernández and Aguirre-Urreta (2005) based on referred material.) Differing from other ophthalmosaurians by the following combination of characters: tooth roots quadrangular (as in many platypterygiines); plicidentine present and well developed in cross-section but not visible on the external surface of the root (plicidentine absent in *Platypterygius australis* (McCoy, 1867); scapula with strap-like shaft (rod-like in *Kyhytysuka sachicarum*, *Platypterygius americanus* (Nace, 1939), *P. australis*, *Platypterygius hercynicus* (Kuhn, 1946), and probably *Platypterygius platydactylus* (Broili, 1907); humerus with three distal facets, including a small facet for an extrazeugopodial element anterior to the radius (unlike in *Brachypterygius*, *Aegirosaurus*, and *P. americanus*); hexagonal intermedium articulating distally with two digits (unlike in *K. sachicarum*, *P. americanus*, *P. australis*, and *P. platydactylus*); rectangular and tightly packed phalanges (as in *Caypullisaurus*, *P. australis*, and *P. platydactylus*); ulnare distally articulating with metacarpal V (as in *Brachypterygius extremus* (Boulenger, 1904) and *Catutosaurus*, but unlike *Caypullisaurus*, *P. australis*, and *P. platydactylus*); multiple postaxial digits (unlike *Brachypterygius extremus*).

Holotype: MLP 79-I-30-1, humerus and partial forelimb (von Huene 1927: 29, fig. 3).

Type locality and age: Cerro Belgrano, Santa Cruz province, Argentina, Río Belgrano Formation (Barremian).

Other referred material: MLP 79-I-30-2 from the type locality (Fernández and Aguirre-Urreta 2005: 585, fig. 2c); TY61 and CPAP-2011-0019 from the Tyndall locality, Zapata Formation.

Occurrence: Santa Cruz Province, Argentina; Tyndall locality (Magallanes, Chile).

Remarks: Reinterpretation of the *Myobradypterygius hauthali* forelimb material. All previous interpretations of *MLP 79-I-30-1* (Huene 1927, Fernández and Aguirre-Urreta 2005, Pardo-Pérez *et al.* 2012) identify the preserved zeugopodial element as the radius, following the preliminary interpretation by von Huene (1925). Here, we follow Campos *et al.* (2024) in considering

this element to be the ulna, based on detailed comparisons between *MLP 79-I-30-1* and the Chilean specimens CPAP-2011-0019 and TY61 (Fig. 3B–G). Given that Campos *et al.* (2024) did not elaborate on their reinterpretation of *MLP 79-I-30-1*, we briefly summarize the reasons here: the proximal carpal distal to the zeugopodial element in *MLP 79-I-30-1* primarily supports one digit rather than two, which is observed in the ulnare but not the radiale in the more complete Chilean material. The radiale in the Chilean *Myobradypterygius hauthali* material has parallel proximal and distal edges, such that its distal facet is oriented anterodistally rather than purely distally as in the ulnare, and thus supports two digits. Von Huene (1925) based his orientation on the logic that the digit, here interpreted as the anterior accessory digit, could not be digit I. The reasons for this interpretation are unclear, but probably relate to the absence of anterior accessory ossicles in the ichthyosaurian taxa with which he was familiar.

Accordingly, we interpret MLP-79-I-30-2 as preserving the posterior portion of the proximal forefin based on the shape of the proximal carpals. This interpretation differs from that proposed by von Huene (1927) but has previously been suggested by Pardo-Pérez *et al.* (2012) and Campos *et al.* (2024).

Referral of the Chilean material

Pardo-Pérez *et al.* (2012) and Stinnesbeck *et al.* (2014) did not refer the forefin CPAP-2011-0019 from the Tyndall locality to *Myobradypterygius hauthali*, despite noting similarities, but it was suggested in the PhD thesis of Pardo-Pérez (2015), among other specimens classified as *Myobradypterygius hauthali* from the Tyndall fossil locality. This referral was later adopted by Campos *et al.* (2024); however, those authors never addressed the morphological differences listed by Pardo-Pérez *et al.* (2012) differentiating the Chilean and Argentinian material. Stinnesbeck *et al.* (2014) referred TY61, a specimen with good exposure of an articulated forefin, to *Myobradypterygius hauthali*, among other specimens, but did not provide a morphological discussion. Given the good preservation and exposure of the TY61 forefin, it is ideal for comparisons with CPAP-2011-0019 and the reoriented type material. This comparison will address: (i) whether *Myobradypterygius hauthali* was present in the Hauterivian of Chile; and (ii) which characteristics cited by Pardo-Pérez *et al.* (2012) appear to be variable intraspecifically.

Pardo-Pérez *et al.* (2012) raised seven key features in which CPAP-2011-2019 differs from *Myobradypterygius hauthali*, which we address in detail here.

(i) A facet for an articulation with a preradial element is absent in the humerus of CPAP-2011-0019, but present in the holotype of *Myobradypterygius hauthali*. This cannot be assessed in CPAP-2011-0019 because the anterior margin is not exposed, but a preradial element articulating with the humerus is present in TY61. In the *Myobradypterygius hauthali* holotype, however, this facet is described as being fairly flat, whereas in TY61 it is clear that it is deeply concave. This difference might be related to superficial erosion of the humerus in TY61.

(ii) The proximal humerus is flattened in CPAP-2011-0019 and TY61, but deeply convex in the holotype of *Myobradypterygius hauthali*. Based on the much larger size of the Tyndall specimens relative to the holotype, this difference is unlikely to be of ontogenetic origin [94 mm long (CPAP-2011-0019), 96 mm long (TY61) vs. 72 mm long (*MLP 79-I-30-1*); Fernández and Aguirre-Urreta 2005, Pardo-Pérez *et al.* 2012]. Moreover, the humerus in the holotype of *Myobradypterygius hauthali* is more massive proximally than distally, although the total width between the two ends is similar (von Huene 1927). The latter is not observed in TY61 but is present in CPAP-2011-0019. The difference between the two Chilean specimens suggests that this character is likely to be an artefact that relates to how the humerus is exposed, and the proximal convexity is likely to be affected by similar factors. Thus, at present, we do not consider these differences to be taxonomically significant. However, further preparation of the Tyndall material might reveal this difference to be of importance.

(iii) CPAP-2011-0019 has one preaxial digit and three postaxial digits with a posterior row of accessory ossicles, whereas the holotype *Myobradypterygius hauthali* has at least three preaxial digits. Based on our proposed reorientation, *MLP 79-I-30-1* preserves one preaxial digit and some anterior accessory ossicles, similar to TY61, which is consistent with the exposed portion of CPAP-2011-0019. At least two postaxial digits are present in the Argentinian *Myobradypterygius hauthali* material, with the number of digits being limited by preservation rather than by morphology. At least two postaxial digits and either a posterior row of accessory ossicles or a third postaxial digit are present in TY61.

(iv) The intermedium has a distal facet for the articulation of distal carpal four that is twice as long as the facet for distal carpal three in CPAP-2011-0019, whereas in *Myobradypterygius hauthali* these facets are subequal in length. This difference is considered here to be part of normal intraspecific variation. The length difference between the facets is much less pronounced in TY61.

(v) Distal carpal three has six articular facets in CPAP-2011-0019, whereas in the holotype of *Myobradypterygius hauthali* there are seven (specimen *MLP 79-I-30-1*), with the additional facet articulating with metacarpal four. In CPAP-2011-0019, distal carpal three articulates with the intermedium, radiale, distal carpal two, metacarpal three, and distal carpal four. A contact with metacarpal two was probably present but substantially reduced. Following reorientation, the elements contacting distal carpal three in *MLP 79-I-30-1* do not differ from the configuration of CPAP-2011-0019, including the probable small contact with metacarpal two. However, the contact between distal carpal three and metacarpal two is absent in TY61, indicating that intraspecific variation in this character is likely.

(vi) The posterior facets of metacarpal three articulate posteroproximally with distal carpal four and posterodistally with metacarpal four in CPAP-2011-0019, which is not the case in *Myobradypterygius hauthali*. After reorientation of *MLP 79-I-30-1*, metacarpal three articulates with both distal carpal four and metacarpal IV, which also holds true for TY61.

(vii) Metacarpal four articulates with six elements in CPAP-2011-0019, whereas in *Myobradypterygius hauthali* it articulates with five. Metacarpal four has been portrayed as articulating with five (Huene 1927) or six (Fernández and Aguirre-Urreta 2005) elements in *Myobradypterygius hauthali*, depending on the observer. However, in *Myobradypterygius hauthali* the posterior facet of metacarpal four contacts the first phalanx of digit five and possibly also the second phalanx but never with metacarpal five. In both CPAP-2011-0019 and TY61, metacarpal four contacts metacarpal five and the first phalanx of digit five, i.e. metacarpal four is situated more proximally in the limb. This change is slight; in all materials, the largest contact is with the first phalanx, and at present, it is considered to represent intraspecific variation.

Based on these observations, both CPAP-2011-0019 and TY61 are here referred to *Myobradypterygius hauthali* (as previously suggested for the former specimen by Campos *et al.* 2024), although further preparation might reveal potential differences in humeral morphology.

Description of TY61: a complete ichthyosaur skeleton including cranium and postcranium

(Fig. 2; Supporting Information, Model S1)

The specimen is exposed from skull to tail in ventrolateral to ventral view and has a total estimated length of 3 m. Glacial erosion has exposed the skull from the narial region to the occipital region. Given that the posterior skull is wider, more bone has been eroded posteriorly, leading to exposure of braincase elements. The anterior rostrum is covered by sediment. Both forefins are exposed in ventral view. The dorsal vertebral column lies inside the matrix, hence only the ventral ends of the ribs are exposed. The anterior part of the caudal vertebral column is also exposed.

Skull

Basioccipital: The ventrolateral exposition of the basioccipital of the specimen TY61 shows a convex occipital condyle and

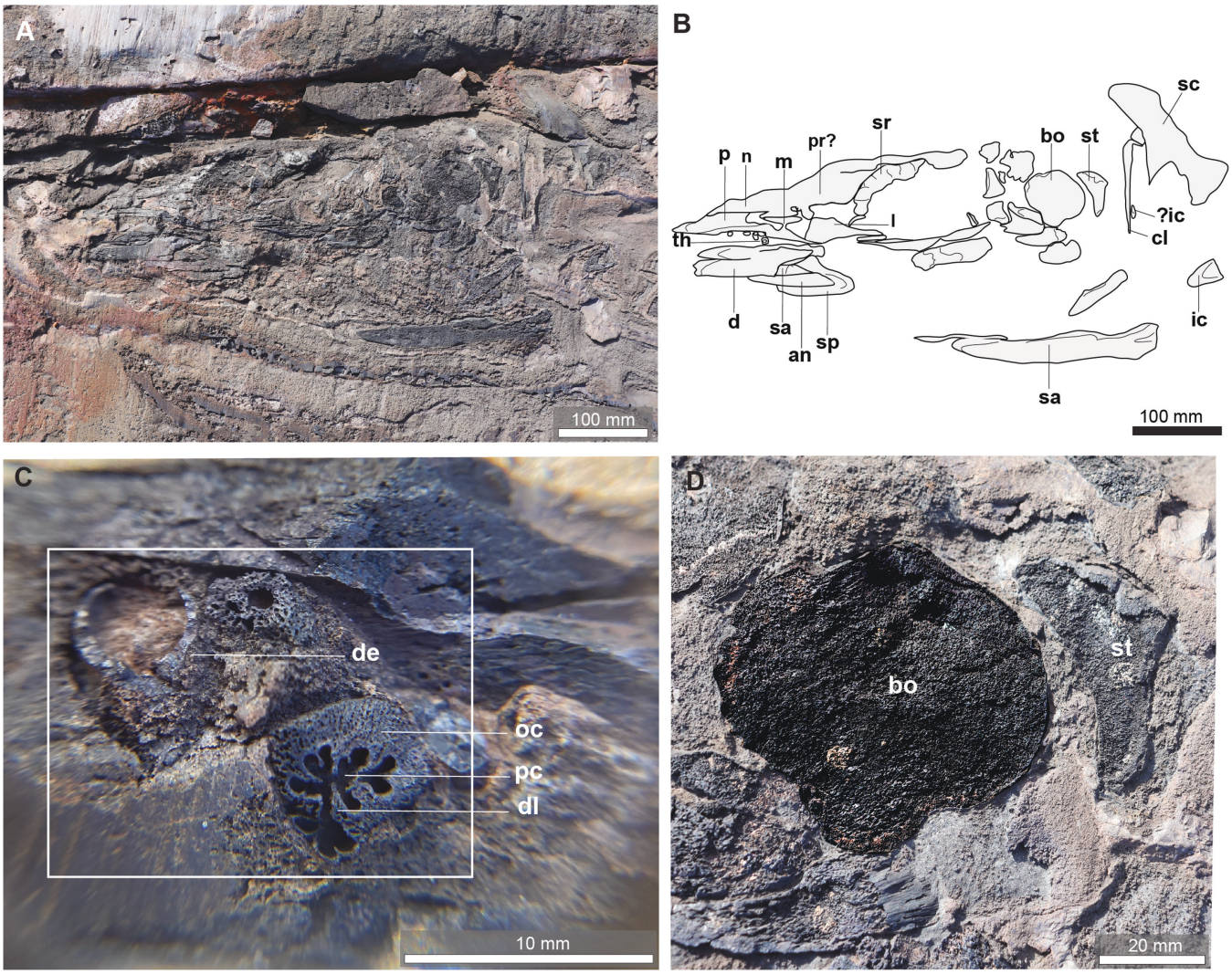

Figure 3. A, B, photograph of the skull and part of the pectoral girdle of TY61 (A) and an interpretative drawing (B). C, a close-up of teeth of TY61. D, a close-up of basioccipital of TY61. Abbreviations: an, angular; bo, basioccipital; cl, clavicula; d, dentary; de, dentine; dl, dentine lamellae; ic, interclavicular; l, lachrymal; m, maxilla; n, nasal; oc, osteocementum; p, premaxilla; pc, plicidentine; sa, surangular; sc, scapula; sp, splenial; st, stapes.

an almost straight anterior margin marked by a groove for the notochordal remnant. A constriction with a diameter of 5 mm marks the separation between the extracondylar area and the condyle (Fig. 3D). The basioccipital is rather long anteroposteriorly, but the extracondylar area is only slightly wider than the occipital condyle. A clear anterolaterally directed facet is visible on the left side of the anterior basioccipital; a similar facet on the right is not as clearly exposed. These facets are interpreted here as stapedial facets.

Stapes: The stapes is rotated 90° from its original position, and it is now located adjacent to the basioccipital condyle. It appears to be preserved in dorsal view. The medial head is anteroposteriorly three times wider than the quadrate facet. The quadrate facet is not expanded relative to the stapedial shaft. The posterior edge of the stapes is concave, and the anterior edge is straight, with the quadrate facet offset by an obtuse angle (Fig. 3D).

Dermatocranium: Additional skull bones are preserved (e.g. the left lacrimal, left sclerotic ring, and left nasal). Despite the quality of preservation appearing to be fairly good, the limited exposure of many of these bones makes identification difficult (Fig. 3A, B). The lacrimal is relatively anteroposteriorly broad. One area of particular interest is the region surrounding the external nares. Although preservation of this region makes interpretation difficult, it appears that the maxilla is dorsoventrally deep, with a broad dorsal process forming an anteroposteriorly elongated contact with the nasal. Although the position and shape of the posterior external narial opening cannot be discerned, this configuration seems likely to result in the complete subdivision of the narial opening. The subnarial process of the premaxilla appears to extend almost as far posteriorly as the nasomaxillary pillar. The anterior maxilla has a short exposure in lateral view relative to the inferred length of the nares (Fig. 3A, B).

Dentition: The maxilla is dentigerous, and several teeth are preserved, although unfortunately, none preserve the enamel. The teeth have quadrangular roots in cross-section, with a thick osteocementum layer covering the dentine. Plicidentine is extremely well developed, although not visible externally on the tooth root (Fig. 3C).

Postcranial axial skeleton: The vertebral column as exposed consists of 21 articulated vertebrae in ventrolateral view (Fig. 2; for measurements, see Supporting Information, Table S1). Some apophyses are visible; however, it is unclear whether these correspond to parapophyses or synapophyses. Neural arches and spines, in addition to most of the ribs, are not exposed. According to the size of the exposed vertebral series and its topographic location in the skeleton, the vertebral segment is likely to represent the posterior dorsal and anterior preflexural caudal vertebral column. The anteriormost vertebrae have a width or height-to-length ratio of 2.2, which decreases rapidly along the exposed length of the preflexural vertebrae and suggests a relatively low degree of vertebral regionalization. The posteriormost section of the last exposed vertebrae is embedded, which suggests that the rest of the caudal series, including the tail bend, are still contained in the sediment. The ventralmost section of 22 dorsal ribs from the right side of the skeleton is exposed. Four ribs lie across the phalanges of the left forefin. Robust gastralia overlap the right forefin; these are arrayed with at least one dorsal and one ventral element per row per side.

Appendicular skeleton

Pectoral girdle: One coracoid is preserved, probably in ventral view. Its poor preservation and incomplete exposure prevent further description. A bone fragment lateral to the coracoid might represent a piece of the right scapula. The left clavicle is also preserved, as a section through the median stem of the interclavicle.

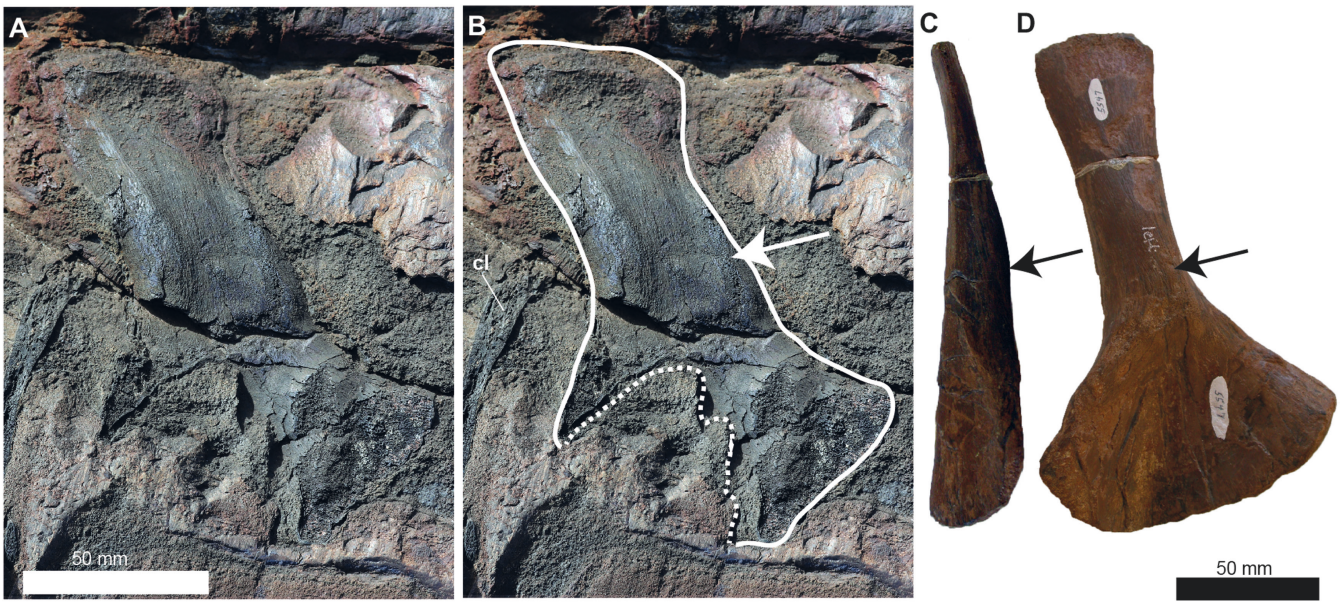

Figure 4. A, B, close-up of the left scapula of TY61 in external view (A) and an interpretation (B). The arrow indicates the slightly concave lateral surface of the shaft. C, D, left scapula of the type specimen of *Platypterygius americanus* (UW 5547) in anterior view (C) and external view for comparison (D). The arrow indicates clear convexity of the shaft distal to the proximal blade. Abbreviation: cl, clavicula.

By far the best-preserved element of the pectoral girdle is the left scapula. It is exposed in external view and is preserved in three dimensions (Fig. 4A). The distal blade of the scapula is strap-like, and the distal-most end is thickened and roughened. The anterior edge is flattened, bearing a prominent facet for the clavicle. The proximal end is concave, and the concavity remains covered in sediment (Fig. 4B). An acromion process is present. Although the glenoid facet is exposed, preservation does not permit an accurate assessment of the relative sizes of the glenoid and coracoid facets.

Forefin: Both forefins of TY61 are exposed in ventral view. The right forefin is preserved more completely than the left one; therefore, the following description is based mainly on the right forefin. The exposed portion of the right forefin measures 261 mm in proximodistal length and 142 mm in anteroposterior width. The distal margins of the distal-most phalanges are not exposed, indicating that the distal-most portion of the forefin continues into the matrix. The forefin bears seven digits (digits II, III, IV, and V, according to Motani 1999, in addition to one preaxial and two postaxial digits), in addition to one row of preaxial and one row of postaxial accessory ossicles. Only a portion of the left forefin of TY61 is exposed. The phalanges are rectangular in shape, but they lie separate from each other. The left forefin shows seven digits (Figs 2, 5F, G).

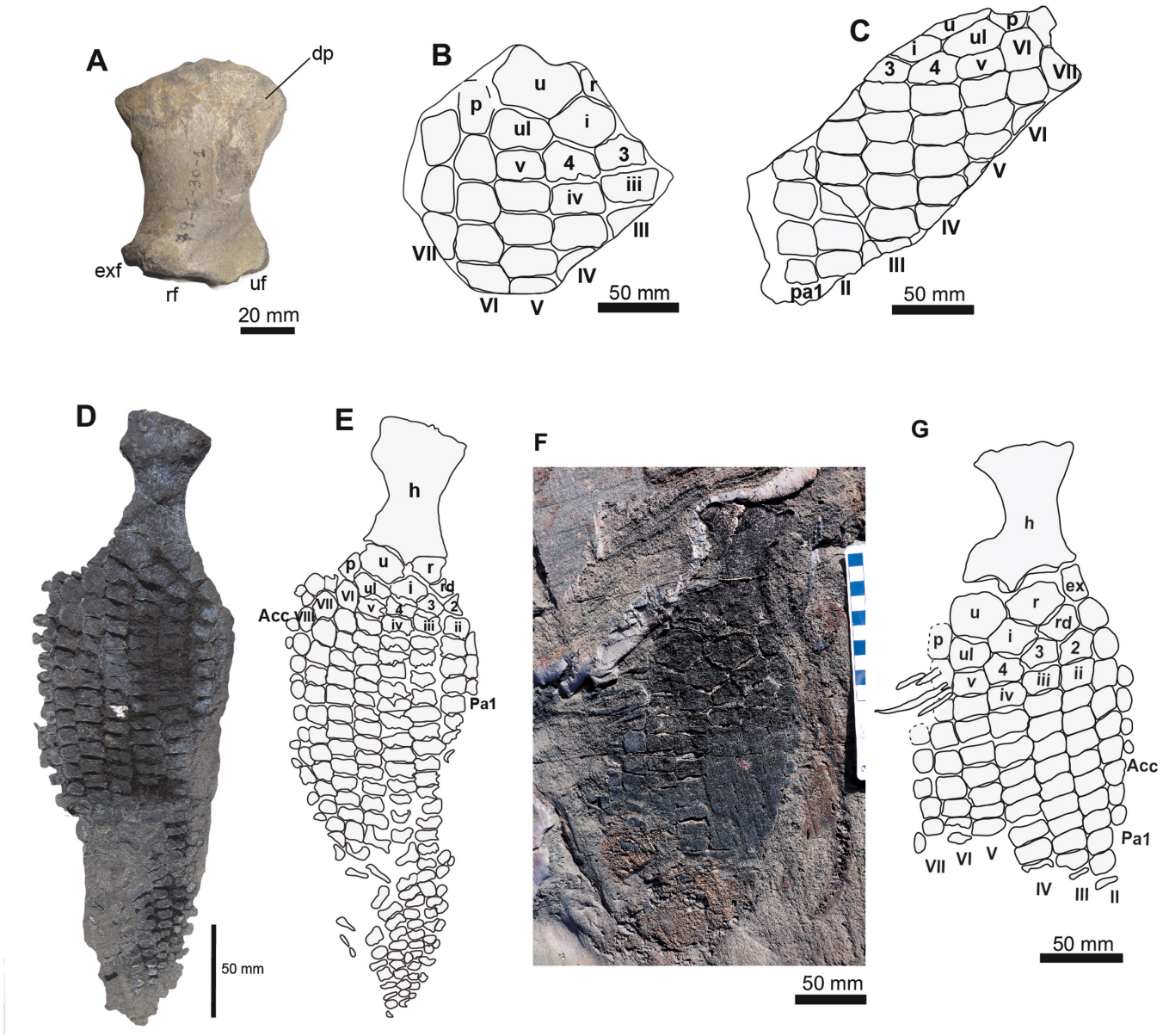

Figure 5. Comparative scheme of *Myobradypterygius hauthali* forefins with Tyndall specimens forefins. A, B, *MLP 79-I-30-1* humerus in dorsal view (A) and fragment of forefin (B). C, MLP 79-I-30-2 fragment of forefin. D, image of CPAP-2011-0019 and interpretation (E). F, image of TY61 and interpretation (G). Abbreviations: acc, anterior accessory phalanges; dp, dorsal process; ex, extrazeugopodial element; exf, extrazeugopodial facet; h, humerus; i, intermedium; II, digit two; III, digit three; IV, digit four; r, radius; ra, radiale; rf, radius facet; p, pisiform; pa1, preaxial digit one; u, ulna; uf, ulna facet; ul, ulnare; V, digit five; VI, digit six; VII, digit seven. Arabic numbers are distal carpals. Lowercase roman numerals are metacarpals. Uppercase roman numerals are digits.

Humerus: The right humerus is exposed in TY61. The humerus is proximodistally longer than its maximum anteroposterior width (96 mm long vs. 76 mm maximum wide), and its distal margin is wider than its proximal one (68 vs. 76 mm). The humerus has three distal articular facets for articulation with the ulna, radius, and an anterior extrazeugopodial element. The facets of the radius and ulna are similar in length, and the facet for the extrazeugopodial element is the shortest one. The three distal articular facets are markedly concave. It is not possible to recognize humeral processes owing to abrasion of the exposed bones. For further details, see the comparisons with CPAP-2011-0019 in the section 'Referral of the Chilean material'.

Zeugopodium: The radius is hexagonal in outline, with the anterior and posterior facets being the shortest. The radius articulates with the humerus proximally, the extrazeugopodial element anteriorly, and the ulna posteriorly. Distally, the radius is divided into two subequal facets forming an angle of 125°. The anterodistal facet articulates with the radiale, and the posterodistal one articulates with the intermedium. The radius is 1.4 times anteroposteriorly wider than its proximodistal length (see Supporting Information, Table S2).

The ulna is roughly pentagonal in outline, and it is proximodistally longer and anteroposteriorly wider than the radius. Proximally, it articulates with the humerus. The anterodistal facet articulates with the intermedium and the posterodistal facet with the ulnare. The ulna articulates posterodistally with the pisiform.

The anterior extrazeugopodial element appears flask shaped and is proximodistally longer than anteroposteriorly wide (22 mm long vs. 13 mm wide). Proximally, it articulates with the distal facet of the humerus. The posterior margin of the anterior extrazeugopodial element articulates with both the radius and the radiale. As preserved, the radius and radiale do not directly contact the extrazeugopodial element. The gap between the bones was probably filled with cartilage or connective tissue. The distal margin of the extrazeugopodial element articulates with the preaxial element of the proximal carpal row.

Taphonomy

The anterior rostrum remains covered by sediment and appears to be directed downwards. However, given that the sedimentary laminae are not horizontal and erosion did not occur parallel to the bedding plane, it is unclear how deeply the skull penetrated into the sediment. The specimen does not show obvious signs of head-first arrival at the seafloor, such as the basioccipital being displaced into the cranial cavity. Additionally, the left forefin, which lies higher in the sediment, is positioned slightly anterior to the lower right forefin, which is inconsistent with a rostrum-first penetration into the sediment (Hofmann 1958). In the caudal region, the sedimentary laminae are evenly draped over the bones. This effect is likely to be attributable to slow sedimentation, but late diagenetic differential compaction cannot be ruled out. The bones themselves maintain a high degree of three-dimensionality.

Results of the phylogenetic analysis

Under equal-weights parsimony, analysis of the matrix of Campos *et al.* (2021) resulted in 3500 most parsimonious trees (MPTs) of length 234. *Myobradypterygius hauthali* was resolved within an unresolved Platypterygiinae clade. IterPCR did not improve resolution of this clade further. The analysis of the matrix of Zverkov and Jacobs (2020) resulted in 148 MPTs of length 430. Platypterygiinae was not resolved as a clade, collapsing into a polytomy at the base of Ophthalmosauria. IterPCR resolved Platypterygiinae as a clade but provided little internal resolution. The analysis of the matrix of Cortés *et al.* (2021) resulted in 60 MPTs of length 303. *Myobradypterygius hauthali* was resolved within Platypterygiinae as part of a clade comprising large platypterygiines with brick-like phalanges, but excluding *Maiaspondylus lindoei* and *Platypterygius platydactylus*. IterPCR resolved the latter species as forming a separate clade near the base of Platypterygiinae, but did not further resolve the position of *Myobradypterygius hauthali* (Supporting Information, Fig. S1).

The results of these three analyses support the conclusion that *Myobradypterygius hauthali* is a platypterygiine ichthyosaur but do not provide additional information on its phylogenetic position.

Under extended implied weighting, with collapse of nodes supported by only one step, resolution was improved considerably for two of the four matrices analysed (Fig. 6A, C). The analysis of the matrix of Zverkov and Jacobs (2020) resulted in three trees of length 17.38712. *Myobradypterygius hauthali* was resolved within Platypterygiinae as sister to the Late Cretaceous taxon *Sisteronia seeleyi*. IterPCR was not required to increase resolution. The analysis of the matrix of Cortés *et al.* (2021) resulted in 51 MPTs of length 12.56302. IterPCR was used to prune three unstable taxa. *Myobradypterygius hauthali* was resolved within Platypterygiinae as part of a clade comprising large platypterygiines with brick-like phalanges, but excluding *Maiaspondylus lindoei* and *P. platydactylus*. Analysis of the matrix of Campos *et al.* (2021) resulted in >10 000 trees of length 9.5921. IterPCR was used to place *Myobradypterygius hauthali* within an unresolved Platypterygiinae clade. Analysis of the matrix of Campos *et al.* (2024) with no rescoring of *Myobradypterygius hauthali* resulted in >10 000 trees of length 24.33043. IterPCR was used to place *Myobradypterygius hauthali* within an unresolved Platypterygiinae clade, but not as either closely related to *Sisteronia* (as in Zverkov and Jacobs) or the large platypterygiines with brick-like phalanges (as by Cortés *et al.* 2021). It is clear that even with the use of extended implied weighting, the three matrices fail to converge on a consensus solution.

Order Ichthyosauria de Blainville, 1835

Family Ophthalmosauria Motani, 1999

Subfamily Ophthalmosaurinae Baur 1887 *sensu* Fischer *et al.* (2012)

Ophthalmosaurinae indet.

Material

TY53: An incomplete specimen preserving cranial and postcranial bones (Fig. 7; Supporting Information, Model S2).

Description

Proportions: TY53 is exposed in left lateral view. The exposed portion is 2.88 m long and constitutes a partly embedded articulated specimen including the skull, a partial axial skeleton, portions of a forefin, the pectoral girdle, and a portion of the pelvic

girdle. Prior to glacial erosion, the specimen probably was virtually complete. The eroded caudal vertebrae of the tail and the complete skull could have measured an additional 2 m. Thus, the animal might have had an estimated total length of 5 m.

Skull: The skull is preserved as three discrete sections, which are cut at different angles and showing perimortem breakage, probably incurred during head-first arrival at the seafloor. These sections are: (i) the anterior rostrum; (ii) nasals and the palate

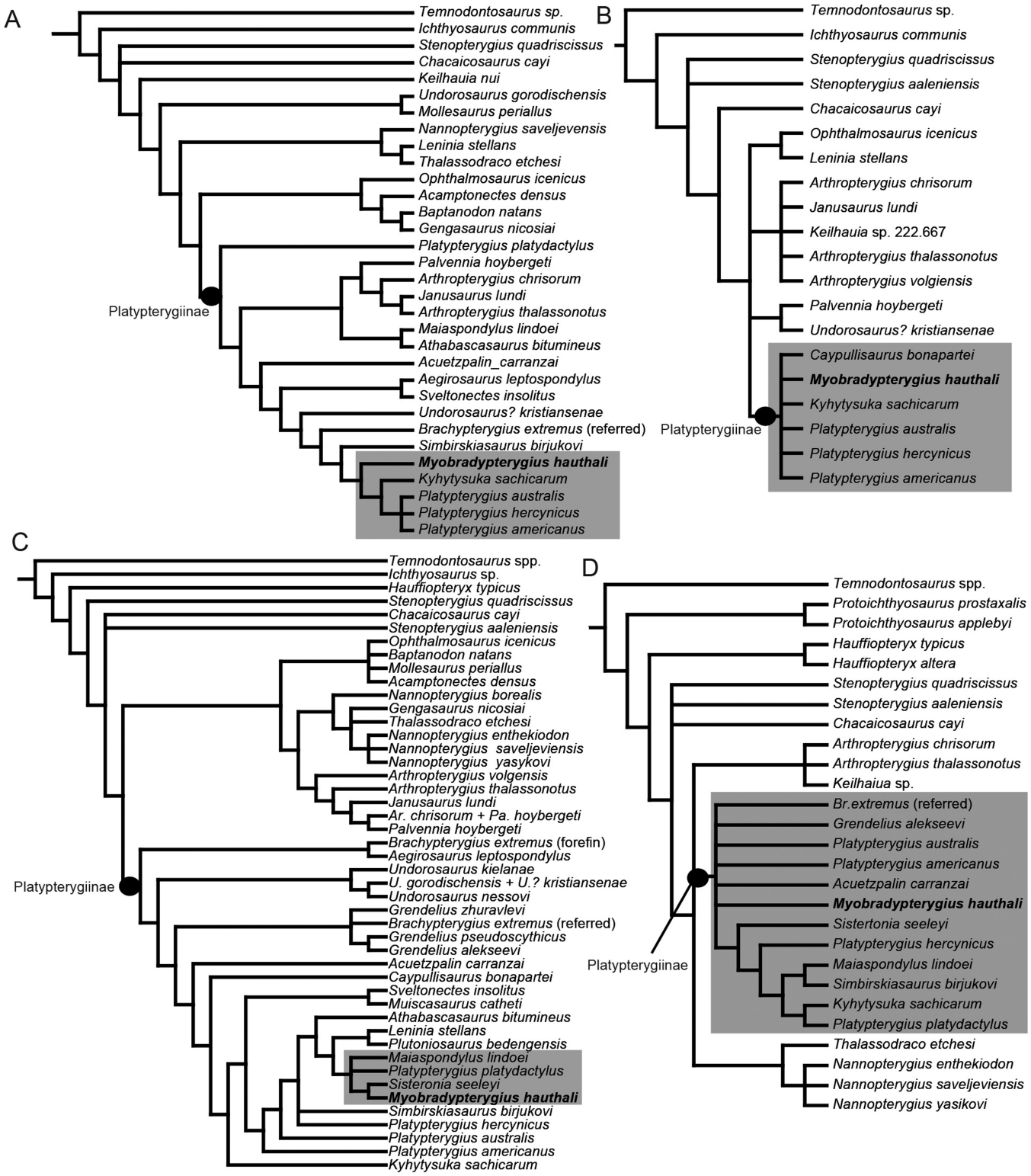

Figure 6. Phylogenetic position of *Myobradypterygius hauthali* under extended implied weighting (k = 12) with unsupported nodes collapsed. Taxon names have been edited to be consistent across authors. A, matrix of Cortés *et al.* (2021). B, matrix of Campos *et al.* (2021). C, matrix of Zverkov and Jacobs (2020). D, matrix of Campos *et al.* (2024) reanalysed without rescoring of *Myobradypterygius hauthali*.

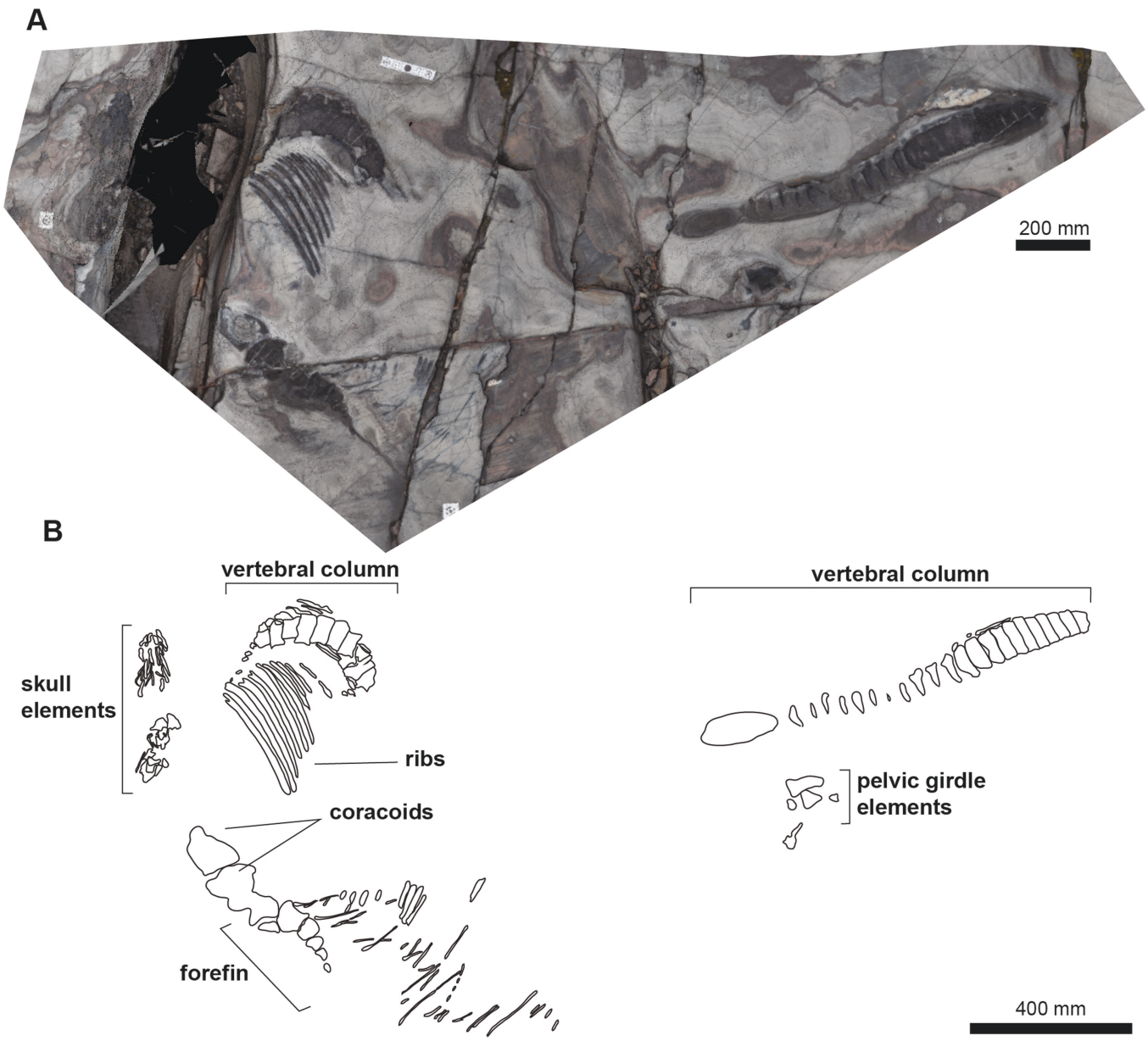

Figure 7. A complete view of the exposed skeleton of TY53. A, image from the photogrammetric reconstruction. B, schematic interpretation.

in the region of the external nares; and (iii) the right lower jaw ramus.

The first segment (i) is from the anterior rostrum. This is preserved in cross-section at a point estimated to be approximately halfway between the orbit and the anterior tip of the rostrum. The best-preserved components are the left premaxilla and nasal. The latter is exceedingly small and forms a right angle in cross-section, forming dorsal and ventral rami. It is likely that the section is close to its anteriormost extent, and is largely, but not entirely, covered by the premaxilla externally. The premaxilla shows a well-developed premaxillary fossa, defined dorsally by a sharp ridge and the alveolar groove. Medial to the alveolar wall, there is an element with an oval cross-section inferred to be a vomer. The right premaxilla and nasal have been abraded at a lower angle and are thus more difficult to interpret. Ventral to the left upper jaw ramus, there is a semicircular structure, which is likely to correspond to the left mandibular ramus. A notch in its lateral margin is interpreted as the dentary fossa, but aside from this, no anatomical information can be extracted.

The rostrum posterior to the cross-section described above has been abraded at an angle near to the horizontal plane. The palate is exposed in dorsal view and appears as a series of elongate, roughly parallel elements. This makes the interpretation of the palate difficult. Posterior to this cluster of bones, however, a broken fragment of the right nasal is preserved, which runs at a slightly different angle to the palate. The nasal fragment must come from the portion anterior to the excavatio internasalis, because it shows a vertically oriented internasal suture and a convex external surface (Fig. 8A, B).

The second skull section (ii) is a posterior section through the rostrum in the region of the external nares. Both nasals are preserved in cross-section. The right one has shifted slightly

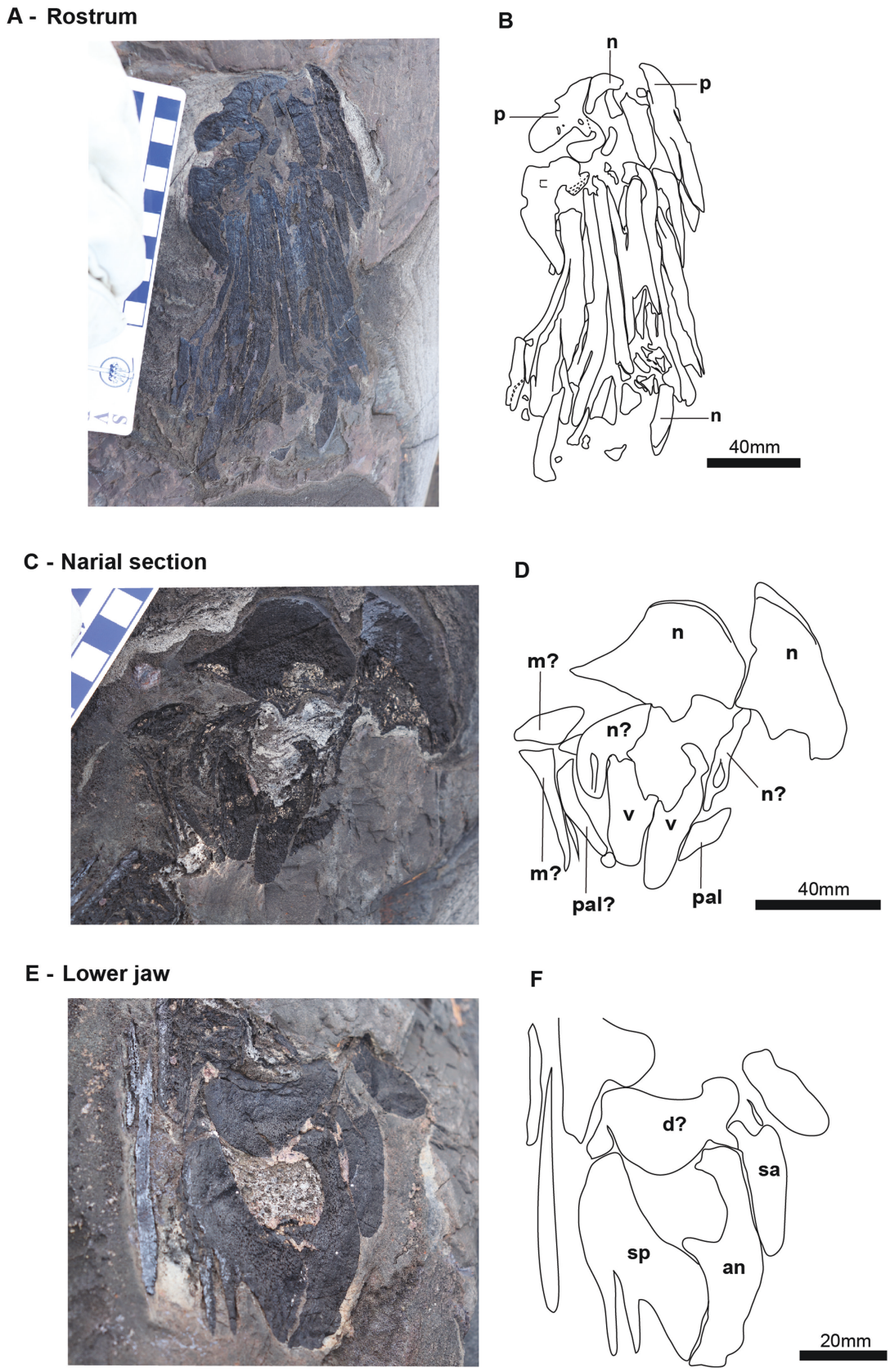

Figure 8. Preserved elements of the skull of TY53 in dorsal view. A, B, rostrum bones (A) and interpretation (B). C, D, narial section (C) and interpretation (D). E, F, lower jaw elements (E) and interpretation (F). Abbreviations: an, angular; d, dentary; m, maxilla; n, nasal; p, premaxilla; pal, palatine; sa, surangular; sp, splenial; v, vomer.

anteriorly relative to the left, such that they are not in articulation nor do they show the same anatomical structures. The right nasal is from a cut anterior to the excavatio internasalis and shows a vertically oriented internasal suture and convex external surface. The left nasal is sectioned across the external narial opening and shows the development of a prominent lateral wing roofing the narial opening. It forms a convex bulge dorsally, indicating a well-developed excavatio internasalis. Both nasals show a compact outer cortex and an extremely spongiose inner surface. Ventral to the nasals is a pair of dorsoventrally deep elements, which are laterally flat and medially concave, forming a tube. These elements articulate with the nasals via a weakly ossified connection and are interpreted as the vomers. On the right, a smaller quadrangular element is preserved, potentially representing the palatine but sectioned almost parallel to the long axis. On the left is a plate-like element, here interpreted as the left palatine in cross-section, and lateral to this is a hatchet-shaped element, potentially part of the maxilla or nasal (Fig. 8C, D).

The third component (iii) is here interpreted as a cross-section through the right mandibular ramus. A round element preserved laterodorsally might represent the right jugal in cross-section, although this is uncertain. The mandible consists of the surangular dorsally and laterally, forming the roof of the Meckelian canal and approximately one-third of the lateral surface of the lower jaw. Ventral and internal to the surangular is the angular, which forms the entire medial wall of the Meckelian canal. The angular forms a robust ventromedial articulation with the splenial. The medial surface of the splenial appears to be pierced by several foramina, which appear as bony projections in section. The dentary has not been identified, although a thin fragment of bone between the lateral and dorsal portions of the surangular might represent its posterior extent. Additional elements exposed ventrolateral to the splenial might represent palatal elements (Fig. 8E, F).

Postcranial axial skeleton: The exposed elements of the postcranium consist of a portion of the anterior dorsal vertebral column with articulated ribs and gastralia, a preflexural portion of the caudal vertebral column, the articulated coracoids, a partial forefin, and pelvic girdle elements (Figs 7, 9). The vertebral column is not completely exposed, but the visible part of the vertebral column is articulated. No apophyses or neural spines are preserved, but a series of 10 articulated centra are associated with dorsal ribs (Fig. 9C, D). The vertebrae are polished owing to erosion, but traces of the dorsal portion of ribs are identified, which covered the vertebrae before being polished by the glacier. Vertebrae increase in length along the preserved series, from 39 mm long in the first centrum where the length can be measured accurately to 46 mm in the last measurable dorsal centrum (for measurements, see Supporting Information, Table S3). The height of the last preserved vertebral centrum is 89 mm, giving a height-to-length ratio of 1.9 for the anterior dorsal region. Posteriorly, 22 articulated preflexural caudal vertebrae are preserved. Anteriorly, the centrum length starts at 40 mm and gradually decreases along the preserved series to 32 mm posteriorly. In contrast, the centrum height of the caudal series begins at 94 mm anteriorly, increases slightly to 105 mm in the tallest centrum, then decreases steadily to 80 mm posteriorly. The maximum height-to-length ratio in the anterior caudal region is 3.2, suggesting a relatively non-regionalized vertebral column.

The dorsal ribs exposed in TY53 are dorsoventrally deep with respect to their anteroposterior length and have an hourglass-shaped cross-section (Fig. 9E). Approximately 27 disarticulated gastralia are also preserved and, based on articulation patterns, were arranged as a dorsal and a ventral element on either side of the body, lacking a medial component. No caudal ribs could be identified.

Appendicular skeleton

Pectoral girdle: The coracoids are preserved in articulation, but glacial abrasion makes the shape difficult to discern with accuracy. They appear to be approximately equidimensional or slightly broader than long. The left coracoid preserves the remnants of an anterior notch. The left coracoid overlaps the proximal margin of the left humerus (Fig. 9A, B).

Forefin: The humerus, zeugopodial elements, and part of the posterodistal fin of one of the two forefins are partly exposed in TY53. Based on embedding position and exposure, this is likely to corresponds to the left forelimb (Fig. 9A, B). The humerus is preserved, possibly in dorsoposterior view. Owing to the twisted embedding angle, little detail can be added.

The radius is only partly exposed, but it is clear that it articulates directly with the anterodorsal margin of the ulna. The radius is ≥53 mm in anteroposterior width and 38 mm in proximodistal length but is not completely exposed. The ulna is completely exposed, possibly in dorsal view, and has a proximodistal length of 72 mm and a maximum anteroposterior width of 69 mm. The posterior margin is concave, indicating that a posterior zeugopodial element was absent. The ulna articulates anterodistally with an anterior mesopodial element (presumably the intermedium, which is not preserved) and distally with the ulnare. The ulnare is proximodistally shorter and anteroposteriorly narrower than the ulna (56 mm wide and 50 mm long). Its posterior margin is rounded, whereas the anterior margin is straight. Distally, a straight margin contacts metacarpal V, which is even shorter and narrower than the ulnare (41 mm wide and 34 mm long). It is posteriorly rounded and is anteriorly concave, although the latter is attributable to erosion. A distally exposed phalanx measures 30 mm in proximodistal length. Its anterior margin is not completely preserved. The distal-most element (a distal phalanx) is the smallest. The exposed section is about twice as proximodistally long as anteroposteriorly wide.

Pelvic girdle: Portions of four bones are exposed in the pelvic girdle area. The largest bone corresponds to the ischiopubis in external view. The ischiopubis is 96 mm in length and 48 mm wide at the medial end; the proximal end is incompletely preserved. The ischiopubis shows a slight constriction at the midpoint and a small foramen at its anterodistal margin. No ischiopubic foramen is observed. A second element preserved next to the ischiopubis is roughly triangular in outline. This bone is tentatively identified as the proximal end of the femur (Fig. 9F, G). The last two bone fragments aligned close to those previously described are indeterminate.

Comparison

TY53 is referred to Ophthalmosaurinae because of the large ulna with a concave and 'edgy' posterior surface (*sensu* Fischer

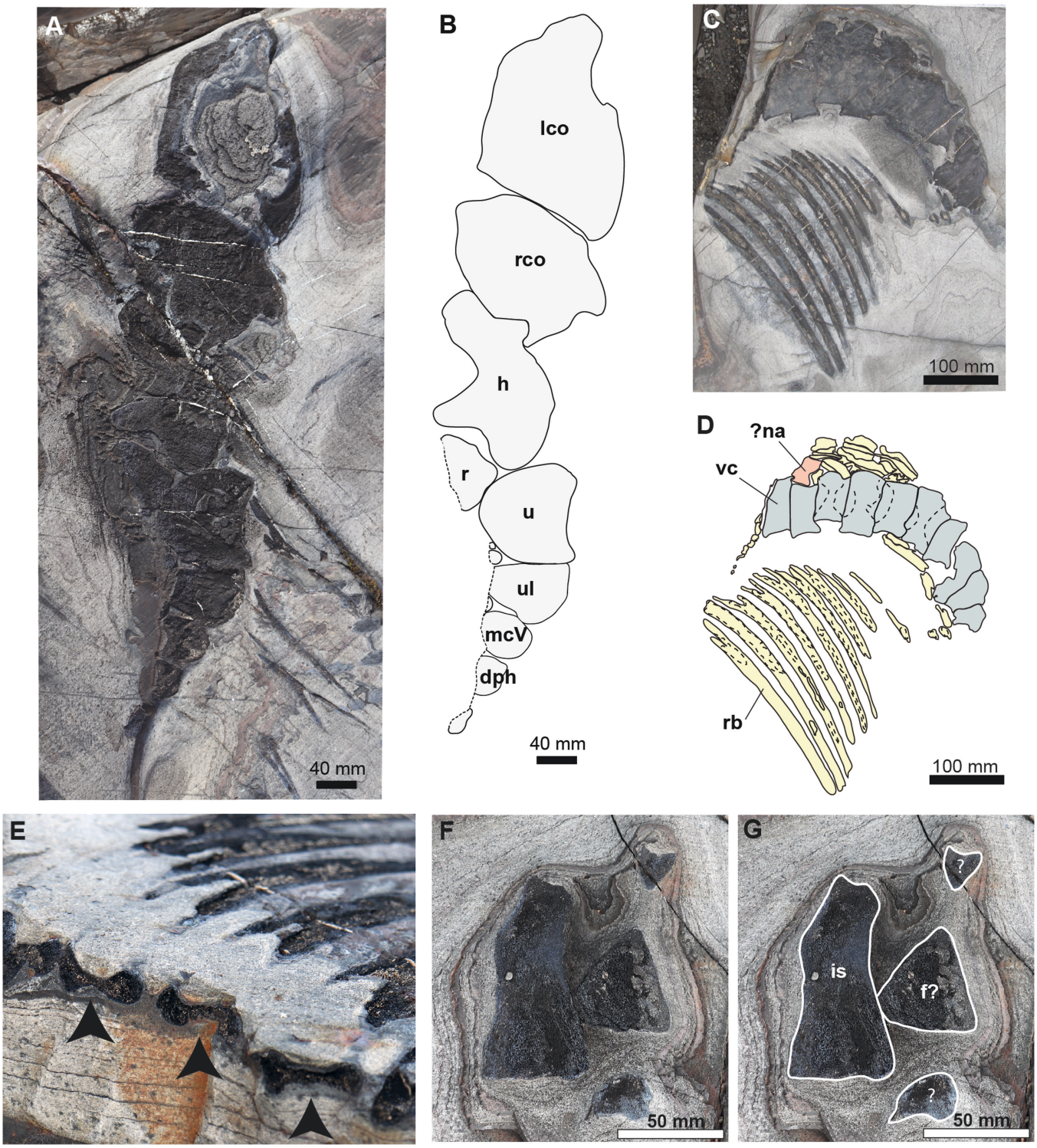

Figure 9. Close-up of preserved anatomical units of TY53. A, B, image of forefin and coracoids (A) and an interpretative drawing (B). C, D, image of preserved vertebral column section with ribs (C) and interpretation (D). E, image showing the prominent eight-shape of ribs in cross-section. F, G, pelvic girdle elements (F) and interpretation (G). Abbreviations: dph, distal phalange; f, femur; h, humerus; is, ischiopubis; lco, left coracoid; mcV, metacarpal five; na, neural arch; r, radius; rb, ribs; rco, right coracoid; u, ulna; ul, ulnare; vc, vertebral column.

et al. 2012). Ichthyosaurs showing this morphology include the Middle–Late Jurassic taxa *Ophthalmosaurus icenicus* (Seeley, 1874; Moon and Kirton, 2016), *Baptanodon natans* (Marsh, 1880), *Nannopterygius* spp. (Zverkov and Jacobs, 2020), *Thalassodraco etchesi* Jacobs and Martill (2020) and the Hauterivian species *Acamptonectes densus* Fischer *et al.* (2012). TY53 also shows rounded forefin elements, as in many of these taxa. *Acamptonectes densus* is the only named ophthalmosaurine from the Valanginian–Barremian interval showing a consistent morphology of the posterior margin of the ulna. However, this

genus clearly differs from TY53 in having ribs that are rounded in cross-section, with a single deep groove (Fischer *et al.* 2012), unlike the clearly hourglass-shaped cross-sections observed in TY53. Therefore, we refer TY53 to Ophthalmosaurinae indet., pending excavation and further preparation.

Taphonomy

According to the preservation of the skeleton, including perimortem fracturing of the skull elements, the angle of the skull relative to the body, and the 'hunch-backed' proximal dorsal

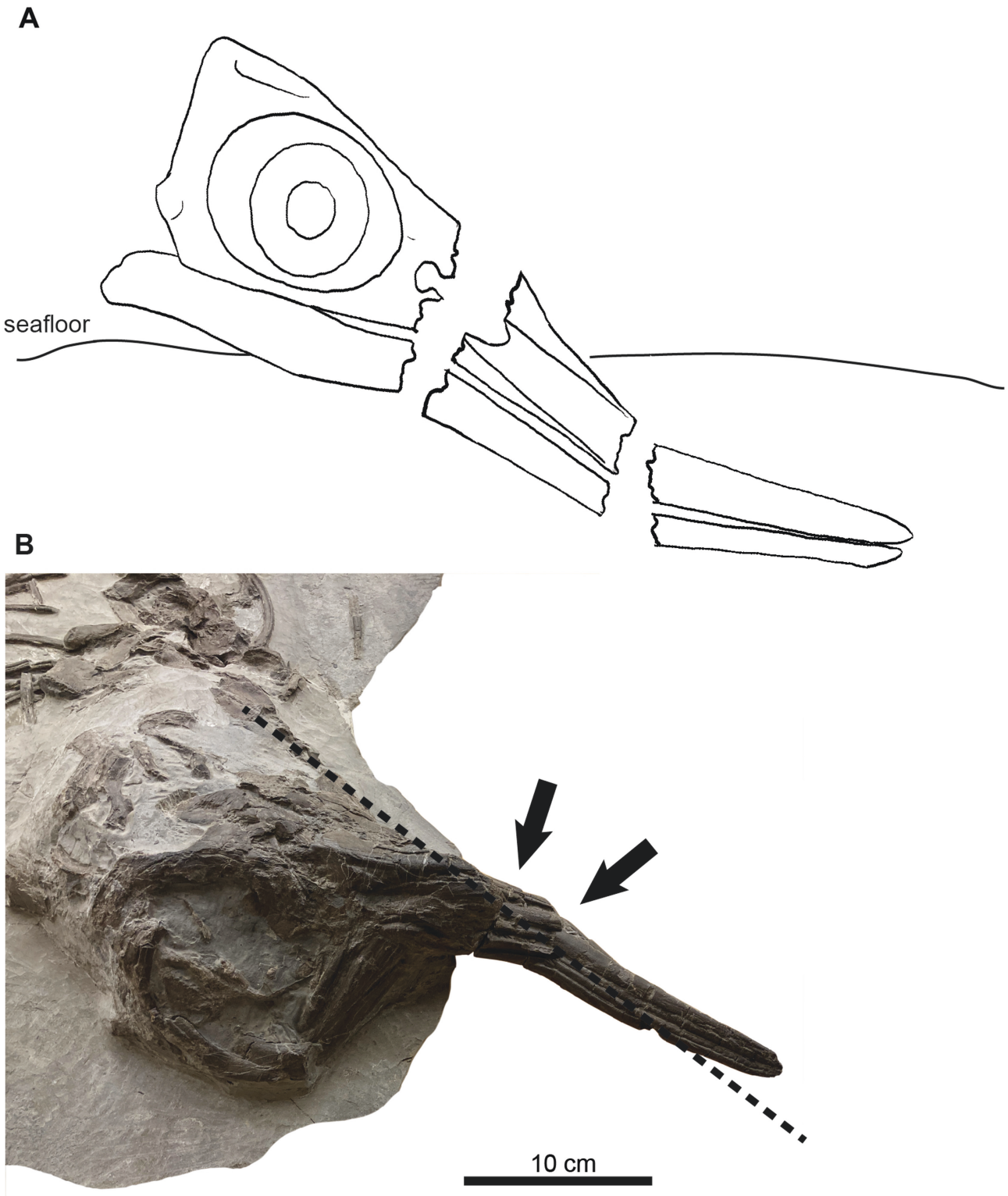

Figure 10. Taphonomical interpretation of TY53. A, sketch indicating in dotted lines the surfaces exposed by glacier erosion after the bone breaks caused by head-first arrival at the seafloor of TY53. B, specimen SMNS 80433 (*Stenopterygius* sp.) as an example of a head-first arrival and broken rostrum in two fragments. The dotted line indicates the exposed margin of the broken portions of the rostrum of TY53.

region (von Huene 1922), a head-first arrival (Wahl 2009) on the probably somewhat soupy (*sensu* Martill 1993) seafloor is plausible. The strength of the fall broke the snout into at least two pieces, which now are exposed in the posterior cross-section and the anterior dorsal-to-cross-sectional view (Fig. 10), suggesting that the soft substrate was thin and underlain by a consolidated seafloor.

DISCUSSION

The problematic genus *Platypterygius*

Platypterygius is a genus that was named more than a century ago and has since been used as a wastebasket for Cretaceous ichthyosaur species (Druckenmiller and Maxwell 2010, Fischer *et al.* 2012, 2014, Zammit 2012, Fischer 2016). Updated studies and new material from different localities have revealed that most of the referred species are not closely related to the type species, originally described based on a single specimen, which was destroyed during World War II (*Platypterygius platydactylus* Broili, 1907). It has been proposed several times that *Platypterygius* should be restricted to the type species only (Fischer *et al.* 2014, 2016) and other '*Platypterygius*' species reassessed to understand their diversity better and avoid the confusing taxonomy caused by this former classification (Cortés *et al.* 2021).

Generic affinities of '*Platypterygius*' *hauthali*

In the early 20th century, fragments of Barremian-aged ichthyosaurs were collected from Santa Cruz Province, Argentina (history reviewed by Fernández and Aguirre-Urreta 2005). Von Huene (1925) mentioned these fragments and later named them as a new genus and species, *Myobradypterygius hauthali* Huene, 1927. In 1972, McGowan suggested that all Early Cretaceous species of ichthyosaurs should be assigned to the genus *Platypterygius*, based on a shared longipinnate forefin structure (i.e. intermedium primarily supporting a single-digit distally). He rejected the genus *Myobradypterygius* arbitrarily but retained the species *Platypterygius hauthali* for all the Neocomian material of South America, despite its latipinnate forefin construction being incompatible with his concept of *Platypterygius*. Until very recently (Campos *et al.* 2024), *Myobradypterygius hauthali* has remained within the genus *Platypterygius*, in large part owing to the extremely fragmentary nature of the type material and lack of any subsequent finds, especially of associated cranial remains.

Campos *et al.* (2024), in their examination of the type material, supported the validity of the genus *Myobradypterygius* based on detailed comparisons of forelimb structure. Our reassessment of '*Platypterygius*' *hauthali* (von Huene, 1927), based on two ichthyosaur specimens recovered from the Tyndall fossil locality, provides additional support for this view based on much more comprehensive skeletal material. Diagnostic cranial and postcranial elements are preserved in specimen TY61. Although the skeleton is unprepared, anatomical details of the articulated skeleton are well preserved and exposed in two dimensions as the sediment matrix was polished by glacier activity. We here report on the morphology of the basioccipital, the tooth root morphology, including plicidentine and a quadrangular cross-section, the subdivided narial opening of TY61, and the strap-like scapular shaft. This adds important new information to the previously unknown skull and scapula of *Myobradypterygius hauthali*. Both TY61 and CPAP-2011-0019 overlap anatomically with von Huene's type and referred material, but TY61 additionally includes cranial remains that allow a detailed assessment of the similarities between *Myobradypterygius hauthali* and the type species of *Platypterygius*, *P. platydactylus*.

Based on new finds from the South of Chile and the cranial and postcranial features described herein, the genus *Myobradypterygius* von Huene, 1927 is recognized as distinct from *Platypterygius platydactylus* Broili, 1907 based on the following series of characters: hexagonal intermedium supporting two digits distally (vs. pentagonal intermedium supporting a single distal digit: Broili 1907); scapular shaft strap-like (vs. rod-like shaft: measurements and illustrations in the study by Broili 1907); an articulation between the humerus and a preaxial element present (vs. only two distal humeral facets present: Broili 1907). According to these characters, both CPAP-2011-0019 and TY61 are referred to *Myobradypterygius hauthali*. We therefore extend both the chronostratigraphical and geographical distribution of the species from the Barremian of Argentina to the Hauterivian of southernmost Chile.

Ophthalmosaurians with rectangular tightly packed phalanges

Among ophthalmosaurians possessing a forefin with rectangular, tightly packed phalanges are *Caypullisaurus bonapartei*, *P. australis* , *P. platydactylus*, *P. hercynicus*, *P. americanus*, *K. sachicarum*, *Maiaspondylus lindoei* Maxwell and Caldwell (2006b) and *Sveltonectes insolitus* Fischer *et al.* (2011) (McGowan 1972, Wade 1984, Maxwell and Caldwell 2006a, Maxwell *et al.* 2019). However, there are differences in the forefin structure of TY61 and CPAP-2011-0019 and the aforementioned ophthalmosaurians.

Myobradypterygius hauthali differs from *P. australis, P. americanus, P. platydactylus, P. hercynicus,* and *K. sachicarum* in that these latter taxa have a pentagonal intermedium, which articulates distally with only one digit. *Platypterygius hercynicus* also has a humerus with four distal articular facets (for the radius and ulna, and for an anterior and posterior accessory element), whereas *P. platydactylus* and *S. insolitus* have only two distal articular facets, for the radius and ulna, and *P. americanus* has three facets, for the radius, ulna, and a postaxial element. *Maiaspondylus lindoei* and *Caypullisaurus bonapartei* have rectangular phalanges, but the humeri of these species have three distal facets, for articulation with the radius, ulna, and a preaxial element; the facet for the last element is similar in length or longer than that for the radius. The quadrangular intermedium articulates distally with only one digit (homologies following Zverkov and Grigoriev 2020 for *Maiaspondylus lindoei*, and Fernández 2001 for *Caypullisaurus bonapartei*). *Sveltonectes insolitus* has a pentagonal intermedium that articulates distally with two digits (Fischer *et al.* 2011).

The intermedium in the forefin of *Myobradypterygius hauthali* is hexagonal, with a vertex situated between the radius and ulna, articulating distally with two digits (digits three and four). This feature is shared with *Catutosaurus gasparinae* and *Sumpalla argentina*, from the Tithonian (Late Jurassic) of Neuquén Province, Northwest Argentinian Patagonia (Campos *et al.* 2021,

Fernández *et al.* 2021). The holotype of *Catutosaurus gasparinae* is a juvenile individual (humerus 55 mm in length in *Catutosaurus gasparinae* vs. 72 mm in length in the *Myobradypterygius hauthali* type material); however, despite this difference in length, the humerus of *Catutosaurus* is wider at midshaft, both relative to its width and in absolute terms, than that of *Myobradypterygius hauthali* (44 vs. 35 mm). In addition, *Catutosaurus* has distal facets on the humerus for articulation with both anterior and posterior accessory elements. In contrast, *Myobradypterygius hauthali* has only an anterior distal facet on the humerus for articulation with an anterior accessory element. Besides this, the forefin of *Catutosaurus* is not preserved distally, which hampers comparisons regarding the number of distal phalanges and its shape. *Catutosaurus gasparinae* also differs in having rounded tooth roots in cross-section, whereas *Myobradypterygius hauthali* has quadrangular cross-sections, which is one of the diagnostic features of platypterygiine ichthyosaurs (Fischer *et al.* 2012). *Sumpalla argentina* differs from *Myobradypterygius hauthali* in the much more acute angle of divergence between the radial and ulnar facets and in the less anteroposteriorly massive proximal end of the humerus. In addition, the tooth roots of *Sumpalla argentina* are rounded in cross-section, as in *Catutosaurus* but unlike in *Myobradypterygius hauthali* (Campos *et al.* 2021).

The presence of *Myobradypterygius hauthali* in the Hauterivian of Chile supports the existence of a distinct genus of platypterygiine ichthyosaurs from southernmost Gondwana. The geographical distribution of this Early Cretaceous taxon was possibly restricted to the southeastern Pacific by climatic barriers (Rogov *et al.* 2017, Brysch 2018).

A large ophthalmosaurine in the Southern Hemisphere

TY53 is classified as an ophthalmosaurine ichthyosaur because of the presence of a large ulna with a concave and edgy posterior surface (*sensu* Fischer *et al.* 2012). Despite temporal co-occurrence, TY53 is distinct from *Acamptonectes densus* from the European Hauterivian based on the hourglass-shaped ribs in cross-section and the total body size. TY53 is larger than *Acamptonectes densus* (total estimated length of 5 m in TY53 vs. 3 m of *Acamptonectes densus*) and is also larger than the sympatric *Myobradypterygius hauthali*, which has an estimated total length of ~3.5 m.

TY53 is characterized by a short but probably robust forefin with massive elements. The vertebral column has larger vertebrae than known specimens of *Myobradypterygius hauthali* (largest preflexural caudal vertebrae 48.8 mm long × 93.5 mm high in TY53 vs. 30 mm long × 65 mm in height/width in TY61) and ribs more than twice as dorsoventrally deep than in specimens of *Myobradypterygius hauthali* here described (29 mm in TY53 vs. 11 mm in TY61).

Both TY53 and *Myobradypterygius hauthali* have been discovered in the same locality and come from the same stratigraphic unit. This indicates that both species shared the same habitat; however gastric contents and functional morphology of the skull and dentition remain too poorly known to investigate whether these genera diverged in diet.

TY53 is temporarily classified as Ophthalmosaurinae indet. until the material can be excavated and prepared, considering the extremely difficult excavations in this locality of Tyndall Glacier in southern Patagonia.

CONCLUSION

Three ichthyosaur specimens are here described from the Hauterivian sediments of the Zapata Formation of Torres del Paine National Park in western southernmost Chile. Two of them are referred to *Myobradypterygius hauthali*, previously known only from the Barremian of Argentinian Patagonia. The new material expands the original diagnosis and extends the chronostratigraphic and geographical distribution of the species. Based on the new descriptions provided here, *Myobradypterygius hauthali* differs from *Platypterygius platydactylus* in forefin construction and scapular morphology and should therefore be considered distinct at the generic level.

The third individual (TY53) was documented in the same lithostratigraphic unit as TY61 and CPAP-2011-0019 in the Zapata Formation. It corresponds to an ophthalmosaurine ichthyosaur, characterized as being one of the largest ophthalmosaurines described to date and sympatric with *Myobradypterygius hauthali*. TY53 represents the first Hauterivian ophthalmosaurine from the Southern Hemisphere and the southernmost record of Ophthalmosaurinae. Moreover, its presence in the faunal assemblage demonstrates that ophthalmosaurines were a globally important component of the ichthyosaur faunas during the Early Cretaceous.

This research increases the knowledge of Early Cretaceous ichthyosaurs from the southern Pacific margin of Gondwana and can lead to new research avenues to investigate ichthyosaur evolution, ecology, and dispersion during the late Mesozoic.

SUPPLEMENTARY DATA

Supplementary data is available at *Zoological Journal of the Linnean Society* online.

ACKNOWLEDGEMENTS

We thank the Corporación Nacional Forestal of Chile and Consejo de Monumentos Nacionales of Chile for providing access to the study area and excavation. We acknowledge the entire palaeontological team of expeditions from 2021 to 2023 (Benjamín and Miguel Cáceres, Andrés Pérez, Sebastián Gallardo, Marko Yurac, Catalina Astete, Héctor Ortíz, Jonathan Kaluza, Diego Cabeza, Carlos Báez, Donald Guichapani, Héctor Bontes, Esteban Beltrán, Marcelo Arévalo, Alvaro Ruíz, Carlos Rebolledo, Gastón Peralta, Tiziana Panizza, José Jimenez, Rodrigo Sebastián Sánchez, Fernando Rey, and Nick Gross) and the logisticians Jone Mungia and Isaac Gurdiel, Tienda de montaña Grado Zero, Wintek Patagonia Aventura, Turismo Vista Paine, the Ilustre Municipalidad de Torres del Paine, DAP airlines, the Chilean Antarctic Institute, the Laboratorio de Ontogenia y Filogenia of Universidad de Chile, UMAGTV, and the Natural History Museum Río Seco (Punta Arenas, Chile) for the logistic support in the organization of the expeditions and in the field. We thank the expedition and excavation team of the years 2009 and 2010. V. Fischer and an anonymous reviewer provided comments that helped to improve the manuscript.

CONFLICT OF INTEREST

All authors declare that they have no conflicts of interest.

FUNDING

J.P.-P. acknowledges the funding support of Deutsche Forschungsgemeinschaft (DFG) Project STI128/15-1 to 3 'Ichthyosaurs of late

Jurassic/early Cretaceous age in the Torres del Paine National Park, Southernmost Chile', the Bundesministerium für Bildung und Forschung (BMBF) research grants 11090223 (2009–2011) and CHL 10A/09, the fellowship from the Deutscher Akademischer Austauschdienst and Consejo Nacional de Ciencia y Tecnología of Chile (DAAD/CONICYT, 2008), and the Stipendien- und Betreuungsprogramm grant (DAAD–STIBET/Uni Heidelberg, 2014) to J.P.-P. D.R.L. also acknowledges support as an 1851 Research Fellow. R.V.-M. is grateful for CHIC ANID FB210018. This research was funded by the Agencia Nacional de Investigación y Desarrollo de Chile (ANID), Project PAI77200036.

DATA AVAILABILITY

Data underlying this article are available in its online supplementary materials. In addition, photogrammetry 3D models of TY61 and TY53 are deposited on Figshare and can be downloaded using the following DOI: 10.6084/m9.figshare.26980975

REFERENCES

Arkhangelsky MS. On the evolution of the forefin skeleton of Ichthyosaurs and the phylogeny of the group. *Voprosy paleontologii i stratigrafii. Nov. ser.(Problems in Paleontology and Stratigraphy. New. Serie) Vopr. Strategy: Paleontol., Nov. Ser: (Saratov)* 1999;**2**:20–37.

Arkhangelsky MS. On a new ichthyosaur of the genus *Otschevia* from the Volgian Stage of the Volga Region near Ulyanovsk. *Paleontological Journal* 2001;**35**:629–34.

Bardet N. Evolution et extinction des reptiles marins au cours du Mèsozoïque. *Palaeovertebrata* 1995;**24**:177–283.

Baur G. Über den Ursprung der Extremitäten der Ichthyopterygia. *Jahresberichte und Mitteilungen des Oberrheinischen geologischen Vereines* 1887;**20**:17–20.

Benson RBJ, Butler RJ. Uncovering the diversification and history of marine tetrapods: ecology influences the effect of geological sampling bias. In: McGowan AJ, Smith AB (eds), *Comparing the Geological and Fossil Records: Implications for Biodiversity Studies.* Bath: Geological Society, London, Special Publications, 2011, 191–208.

Blainville HMD. Description de quelques espèces de reptiles de la Californie, précédée de l'analyse d'une système générale d'Erpetologie et d'Amphibiologie. *Nouvelles annales du Muséum d'histoire naturelle* 1835;**4**:233–96.

Bouma AH. *Sedimentology of Some Flysch Deposits*. Amsterdam: Elsevier, 1962.

Broili F. Ein neuer Ichthyosaurus aus der norddeutschen Kreide. *Palaeontographica* 1907;**54**:139–62.

Brysch, S. Changes in climate and palaeoenvironment during the Late Jurassic–Early Cretaceous in southern South America and western Antarctica. PhD Thesis, Ruprecht-Karls Universität Heidelberg, 2018.

Campos L, Fernández MS, Bosio V *et al.* Revalidation of *Myobradypterygius hauthali* Huene, 1927 and the phylogenetic signal within the ophthalmosaurid (Ichthyosauria) forefins. *Cretaceous Research* 2024;**157**:105818. https://doi.org/10.1016/j.cretres.2023.105818

Campos L, Fernández MS, Herrera Y. A new ichthyosaur from the Late Jurassic of northwest Patagonia (Argentina) and its significance for the evolution of the narial complex of the ophthalmosaurids. *Zoological Journal of the Linnean Society* 2020;**188**:180–201.

Campos L, Fernández MS, Herrera Y *et al.* Morphological disparity in the evolution of the ophthalmosaurid forefin: new clues from the Upper Jurassic of Argentina. *Papers in Palaeontology* 2021;**7**:1995–2020. https://doi.org/10.1002/spp2.1374

Cignoni P, Callieri M, Corsini M *et al.* MeshLab: an open-source mesh processing tool. *Sixth Eurographics Italian Chapter Conference* 2008, 129–36.

Cortés D, Maxwell EE, Larsson HC. Re-appearance of hypercanivore ichthyosaurs in the Cretaceous with differentiated dentition: revision of '*Platypterygius*' *sachicarum* (Reptilia: Ichthyosauria, Ophthalmosauridae) from Colombia. *Journal of Systematic Palaeontology* 2021;**19**:969–1002.

Cortés D, Maxwell EE, Larsson HCE *et al.* Ichthyosaur trophic guilds from the Early Cretaceous Paja Formation of Colombia. *8th International Meeting on Mesozoic Fishes and Aquatic Tetrapods Abstract Volume* 2023, 17.

Dalziel IW, de Wit MJ, Palmer KF. Fossil marginal basin in the southern Andes. *Nature* 1974;**250**:291–4.

Druckenmiller PS, Maxwell EE. A new Lower Cretaceous (lower Albian) ichthyosaur genus from the Clearwater Formation, Alberta, Canada. *Canadian Journal of Earth Sciences* 2010;**47**:1037–53. https://doi.org/10.1139/e10-028

Fernández MS. Dorsal or ventral? Homologies of the forefin of *Caypullisaurus* (Ichthyosauria: Ophthalmosauria). *Journal of Vertebrate Paleontology* 2001;**21**:515–20. https://doi.org/10.1671/0272-4634(2001)021[0515:dovhot]2.0.co;2

Fernández MS. Ichthyosauria. In: Gasparini Z, Salgado L, Coria RA (eds), *Patagonian Mesozoic Reptiles*. Bloomington: Indiana University Press, 2007, 271–91.

Fernández M, Aguirre-Urreta B. Revision of *Platypterygius hauthali* von Huene, 1927 (Ichthyosauria: Ophthalmosauridae) from the Early Cretaceous of Patagonia, Argentina. *Journal of Vertebrate Paleontology* 2005;**25**:583–7.

Fernández MS, Campos L, Maxwell EE *et al. Catutosaurus gaspariniae*, gen. et sp. nov. (Ichthyosauria, Thunnosauria) of the Upper Jurassic of Patagonia and the evolution of the ophthalmosaurids. *Journal of Vertebrate Paleontology* 2021;**41**:e1922427.

Fernández MS, Talevi M. Ophthalmosaurian (Ichthyosauria) records from the Aalenian–Bajocian of Patagonia (Argentina): an overview. *Geological Magazine* 2014;**151**:49–59. https://doi.org/10.1017/s0016756813000058

Fischer V. Taxonomy of *Platypterygius campylodon* and the diversity of the last ichthyosaurs. *PeerJ* 2016;**4**:e2604. https://doi.org/10.7717/peerj.2604

Fischer V, Arkhangelsky MS, Naish D *et al. Simbirskiasaurus* and *Pervushovisaurus* reassesed: implications for the taxonomy and cranial osteology of Cretaceous Platypterygiinae ichthyosaurs. *Zoological Journal of the Linnean Society* 2014;**171**:822–41. https://doi.org/10.1111/zoj.12158

Fischer V, Bardet N, Benson RBJ *et al.* Extinction of fish-shaped marine reptiles associated with reduced evolutionary rates and global environmental volatility. *Nature Communications* 2016;**7**:10825. https://doi.org/10.1038/ncomms10825

Fischer V, Maisch MW, Naish D *et al.* New Ophthalmosaurid ichthyosaurs from the European Lowe Cretaceous demonstrate extensive ichthyosaur survival across the Jurassic–Cretaceous boundary. *PLoS One* 2012;**7**:e29234.

Fischer V, Masure E, Arkhangelsky MS *et al.* A new Barremian (Early Cretaceous) ichthyosaur from western Russia. *Journal of Vertebrate Paleontology* 2011;**31**:1010–25. https://doi.org/10.1080/02724634.2011.595464

Goloboff PA. Extended implied weighting. *Cladistics* 2014;**30**:260–72. https://doi.org/10.1111/cla.12047

Goloboff PA, Morales Martín E, Morales ME. TNT version 1.6, with a graphical interface for MacOS and Linux, including new routines in parallel. *Cladistics* 2023;**39**:144–53. https://doi.org/10.1111/cla.12524

Goloboff PA, Torres A, Arias JS. Weighted parsimony outperforms other methods of phylogenetic inference under models appropriate for morphology. *Cladistics* 2018;**34**:407–37. https://doi.org/10.1111/cla.12205

Griwodz C, Gasparini S, Calvet L *et al.* AliceVision Meshroom: an open-source 3D reconstruction pipeline. In: *Proceedings of the 12th ACM Multimedia Systems Conference*, June 2021, 2021, 241–7.

Hofmann J. Einbettung und Zerfall der Ichthyosaurier im Lias von Holzmaden. *Meyniana* 1958;**6**:10–55.

Jacobs ML, Martill DM. A new ophthalmosaurid ichthyosaur from the Upper Jurassic (Early Tithonian) Kimmeridge Clay of Dorset, UK,

with implications for Late Jurassic ichthyosaur diversity. *PLoS One* 2020;**15**:e0241700. https://doi.org/10.1371/journal.pone.0241700

Laboury A, Bennion RF, Thuy B *et al*. Anatomy and phylogenetic relationships of *Temnodontosaurus zetlandicus* (Reptilia: Ichthyosauria). *Zoological Journal of the Linnean Society* 2022;**195**:172–94. https://doi.org/10.1093/zoolinnean/zlab118

Malkowski MA, Grove M, Graham SA. Unzipping the Patagonian Andes—long-lived influence of rifting history on foreland basin evolution. *Lithosphere* 2016;**8**:23–8. https://doi.org/10.1130/l489.1

Mallison H, Wings O. Photogrammetry in paleontology, a practical guide. *Journal of Paleontological Techniques* 2014;**12**:1–31.

Martill DM. Soupy substrates: a medium for the exceptional preservation of ichthyosaurs of the Posidonia Shale (Lower Jurassic) of Germany. *Kaupia* 1993;**2**:77–97.

Maxwell EE, Caldwell MW. Evidence of a second species of the ichthyosaur *Platypterygius* in North America: a new record from the Loon River Formation (Lower Cretaceous) of northwestern Canada. *Canadian Journal of Earth Sciences* 2006a;**43**:1291–5. https://doi.org/10.1139/e06-029

Maxwell EE, Cortés D, Patarroyo P *et al*. A new specimen of *Platypterygius sachicarum* (Reptilia: Ichthyosauria) from the Early Cretaceous of Colombia and its phylogenetic implications. *Journal of Vertebrate Paleontology* 2019;**39**:e1577875.

McGowan C. The systematics of Cretaceous ichthyosaurs with particular reference to the material from North America. *Contributions to Geology* 1972;**1**:9–29.

Moon BC, Kirton AM. Ichthyosaurs of the British Middle and Upper Jurassic. Part 1, *Ophthalmosaurus*. *Monographs of the Palaeontological Society* 2016;**170**:1–84.

Motani R. On the evolution and homologies of ichthyopterygian forefins. *Journal of Vertebrate Paleontology* 1999;**19**:28–41.

Mujal E, Marchetti L, Schoch RR *et al*. Upper Paleozoic to Lower Mesozoic tetrapod ichnology revisited: photogrammetry and relative depth pattern inferences on functional prevalence of autopodia. *Frontiers in Earth Science* 2020;**8**:248.

Pardo-Pérez J. Ichthyosaurs from the Early Cretaceous (Hauterivian – Barremian) from the western border of the Tyndall Glacier Torres del Paine National Park, Southernmost Chile. PhD Thesis, Ruprecht-Karls Universität Heidelberg, 2015.

Pardo-Pérez J, Frey E, Stinnesbeck W *et al*. An ichthyosaurian forefin from the Lower Cretaceous Zapata Formation of southern Chile: implications for morphological variability within *Platypterygius*. *Palaeobiodiversity and Palaeoenvironments* 2012;**92**:287–94. https://doi.org/10.1007/s12549-012-0074-8

Pol D, Escapa IH. Unstable taxa in cladistic analysis: identification and the assessment of relevant characters. *Cladistics* 2009;**25**:515–27. https://doi.org/10.1111/j.1096-0031.2009.00258.x

Rogov MA, Ershova VB, Shchepetova EV *et al*. Earliest Cretaceous (late Berriasian) glendonites from Northeast Siberia revise the timing of initiation of transient Early Cretaceous cooling in the high latitudes. *Cretaceous Research* 2017;**71**:102–12.

Stern CR, De Wit MJ. Rocas Verdes ophiolites, southernmost South America: remnants of progressive stages of development of oceanic-type crust in a continental margin back-arc basin. *Geological Society, London, Special Publications* 2003;**218**:665–83. https://doi.org/10.1144/gsl.sp.2003.218.01.32

Stinnesbeck W, Frey E, Rivas L *et al*. A Lower Cretaceous ichthyosaur graveyard in deep marine slope channel deposits at Torres del Paine National Park, southern Chile. *Geological Society of America Bulletin* 2014;**126**:1317–39.

von Huene, F. F. Die Ichthyosaurier des Lias und ihre Zusammenhänge. 114 pp., 22 pls, Verlag von Gebrüder Borntraeger, Berlin, 1922.

Von Huene F. Ichthyosaurier aus der Kreide Argentiniens. *Revista del Museo de La Plata* 1925;**28**:234–8.

Von Huene F. Beitrag zur Kenntnis mariner mesozoischer Wirbeltiere in Argentinien. *Centralblatt für Mineralogie, Geologie und Paläontologie, B* 1927;**1927**:22–9.

Wade M. *Platypterygius australis*, and Australian Cretaceous ichthyosaur. *Lethaia* 1984;**17**:99–113. https://doi.org/10.1111/j.1502-3931.1984.tb01713.x

Wahl WR. Taphonomy of a nose dive: bone and tooth displacement and mineral accretion in an ichthyosaur skull. *Paludicola* 2009;**7**:107–16.

Wilson TJ. Transition from back-arc to foreland basin development in the southernmost Andes: stratigraphic record from the Ultima Esperanza District, Chile. *Geological Society of America Bulletin* 1991;**103**:98–111. https://doi.org/10.1130/0016-7606(1991)103<0098:tfbatf>2.3.co;2

Zammit M. Cretaceous ichthyosaurs: dwindling diversity or the empire strikes back? *Geosciences* 2012;**2**:11–24. https://doi.org/10.3390/geosciences2020011

Zverkov NG. A problem of naming of the families of Late Jurassic and Cretaceous ichthyosaurs. *Paleontological Journal* 2022;**56**:463–70.

Zverkov NG, Grigoriev DV. An unrevealed lineage of platypterygiines (Ichthyosauria) with peculiar forefin structure and semiglobal distribution in the mid-Cretaceous (Albian–Cenomanian). *Cretaceous Research* 2020;**115**:104550. https://doi.org/10.1016/j.cretres.2020.104550

Zverkov NG, Jacobs ML. Revision of *Nannopterygius* (Ichthyosauria: Ophthalmosauridae): reappraisal of the 'inaccessible' holotype resolves a taxonomic tangle and reveals an obscure ophthalmosaurid lineage with a wide distribution. *Zoological Journal of the Linnean Society* 2020;**191**:228–75. https://doi.org/10.1093/zoolinnean/zlaa028